universe

IMPACT FACTOR 2.813

CITESCORE 3.2

Review

Swift/UVOT: 18 Years of Long GRB Discoveries and Advances

Sam Oates

Special Issue

18 Years of Science with the Neil Gehrels Swift Observatory's Ultra-Violet/Optical Telescope

Edited by

Dr. Peter Roming and Dr. Michael Siegel

MDPI

https://doi.org/10.3390/universe9030113

universe

MDPI

Review

Swift/UVOT: 18 Years of Long GRB Discoveries and Advances

Sam Oates

School of Physics and Astronomy & Institute for Gravitational Wave Astronomy, University of Birmingham, Birmingham B15 2TT, UK; s.r.oates@bham.ac.uk or samantha.oates@ucl.ac.uk

Abstract: The Neil Gehrels Swift Observatory (*Swift*) has been in operation for 18 years. The Ultra-Violet/Optical Telescope (UVOT) onboard *Swift* was designed to capture the earliest optical/UV emission from gamma-ray bursts (GRBs), spanning the first few minutes to days after the prompt gamma-ray emission. In this article, we provide an overview of the long GRBs (whose prompt gamma-ray duration is >2 s) observed by the *Swift*/UVOT, and review the major discoveries that have been achieved by the *Swift*/UVOT over the last 18 years. We discuss where improvements have been made to our knowledge and understanding of the optical/UV emission, particularly the early optical/UV afterglow.

Keywords: gamma-ray burst: general; gamma-ray burst: individual; ultraviolet: general

Citation: Oates, S. Swift/UVOT: 18 Years of Long GRB Discoveries and Advances. *Universe* **2023**, *9*, 113. https://doi.org/10.3390/universe9030113

Academic Editors: Peter Roming and Michael Siegel

Received: 4 January 2023
Revised: 15 February 2023
Accepted: 16 February 2023
Published: 22 February 2023

1. Introduction

Gamma-ray bursts (GRBs) are brief, intense flashes of gamma-rays, often accompanied by a longer-lasting emission in the X-ray to radio wavelengths. The duration of the gamma-ray emission may be as short as a few milliseconds or may last for as long as several hundreds of seconds, during which the GRB 'outshines' all objects in the known universe. The initial gamma-ray emission is followed by an afterglow, longer-lived emission that is usually observed from X-ray through to radio wavelengths [1,2].

GRBs can be divided approximately into two classes, short and long, by the duration of their gamma-ray emissions, with the division at ∼2 s [3]. The short GRBs are thought to be a result of the merger of two compact objects, either two neutron stars or a neutron star and a black hole [4,5]. This was recently confirmed (in one case) with the detection of a GRB associated with the GW signal of binary neutron star merger (GW 170817/AT2017gfo; e.g., [6–10]). Long GRBs are thought to be the collapse of massive stars [11,12]; evidence for this is the association of supernovae a few days after the gamma-ray emission (e.g., [13–16]).

Following the launch of the Neil Gehrels Swift Observatory (henceforth, *Swift*; [17]), it was shown that the empirical categorisation of short and long GRBs, by their gamma-ray duration, quantified by the T_{90} parameter (T_{90} is the time interval over which 90% of the gamma-ray emission is measured) with a division at 2 s, is too simplistic. There is likely some natural overlap in duration between the classes [18]. Some GRBs that are categorised as long or short have been shown to have other properties that suggest that they belong to the other class. The prototypical event was the *Swift* discovered-GRB 060604 [19–22]. More recent examples of each type are GRB 200826A [23–25] and GRB 211211A [26–28]. In addition, different detectors with different sensitivities and different methods for determining T_{90} may result in slightly different values for T_{90}, adding to the complication of classifying GRBs solely by their duration (e.g., [18,29–31]). Because of such complications, there is some preference to categorise GRBs by their progenitors, into merger and collapsar categories, which avoids the pitfalls of classifying GRBs by their gamma-ray durations. However, classifying GRBs into merger (Type I) and collapsar (Type II) classes [32] does often require a more involved analysis and may not be possible for all observed GRBs, for instance, due to insufficient observations. For simplicity, in this review, I will use the empirical short and long GRB dichotomy unless otherwise stated.

In this review, I will discuss the advances in long GRBs and their afterglows as a result of optical/UV observations performed by the Ultra-violet/optical telescope (UVOT) onboard *Swift*. The review is divided into Section 2, a discussion of the discovery and status of long GRBs before the launch of *Swift*; Section 3, an overview of long GRBs observed with *Swift*/UVOT; Section 4, advances in our understanding of the optical/UV emission as a result of *Swift*/UVOT; and summarise in Section 5. A review of short GRBs observed by *Swift*/UVOT is provided in an accompanying article in this special issue.

2. Long GRBs Pre-*Swift*

In this section, to put *Swift*/UVOT and its discoveries into context and where it fits into the timeline of long GRB discoveries, I provide a short overview of our understanding of long GRBs up until the launch of *Swift*.

2.1. The Discovery of GRBs

Gamma-ray bursts were initially detected during the late 1960s by the 4 Vela spacecraft [33]. These unknown sources of gamma-rays were found not to be associated with any object within our solar system, and therefore were assumed to be of Galactic or extra-galactic origin. Further progress had to wait until the launch of the Compton Gamma Ray Observatory (CGRO) in 1992, where, using the Burst Alert Transient Source Experiment (BATSE) onboard the CGRO, it was found that the distribution of GRBs was isotropic, suggesting a cosmological origin [34]. Also discovered using BATSE was the bimodal distribution of the duration of the gamma-ray emission: GRBs with hard spectra and of $<$2 s duration were classified as short-hard GRBs, and those with soft spectra and of $>$2 s duration were classified as long-soft GRBs [3], providing the first evidence for two different types of progenitors.

Emission at longer wavelengths, X-ray to radio, was predicted. This emission, the 'afterglow', was expected to be longer lived and to be observed shortly after the prompt gamma-ray emission [35–37]. A detection was only achieved at longer wavelengths, with the launch of BeppoSax in 1996, which had instruments to observe 0.1–300 keV X-rays [38–41]. The first GRB to be detected in X-rays, and subsequently in the optical, was GRB 970228 [42,43]. Observations of GRB 970508 provided the first redshift, $0.835 \leq z \leq 2.3$ [44], confirming the extra-galactic origin of these sources, and provided the first indications of how energetic these sources are, with an isotropic energy of 7×10^{51} erg calculated for this GRB [44]. One last further major development was the detection of supernovae coincident with long GRBs; the first was SN1998bw, associated with GRB 980425 [13,45]; and the second, SN2003dhm associated with GRB 030329 [15]. With GRB 980425, there was some concern that the supernova was a chance coincidence, but with a second GRB associated with a supernova, the connection between the collapse of massive stars and long GRBs was solidified [16].

2.2. Expectations and Observations of Long GRBs, Pre-Swift

Prior to the launch of *Swift*, the theoretical understanding of long GRBs and their emission in the optical/IR was well developed. The collapse of the massive star to a black hole was predicted to result in the production of relativistic bipolar jets [46]. The relativistic jets can be regarded as a series of relativistic shells with varying Lorentz factors [47,48], which result in internal shocks when the shells with high Lorentz factors catch up with shells of lower Lorentz factor that were emitted earlier. The internal shocks produce the prompt gamma-ray emission. Once the relativistic jet reaches the external medium and ploughs into it, it begins to slow down and produces the external shocks, which comprise of a forward and a reverse shock [1]. The forward shock propagates into the external medium, while the reverse shock travels back through the relativistic ejecta. The emission produced in both shocks is released by synchrotron radiation. This emission results in a long-lived afterglow, which for the most part is emission from the forward shock. The emission produced by the external shocks can be described by power-laws for both the

observed spectra and the light curves. The temporal and spectral indices, α and β, are given using the standard convention of $F(t) \propto t^{\alpha}\nu^{\beta}$, where t is time and ν is frequency. The expected value of the spectral and temporal indices can be described analytically by a set of closure relations [2]. For a given observing band, the choice of closure relation depends on its location relative to the synchrotron frequencies (the synchrotron cooling frequency ν_c, the synchrotron peak frequency ν_m, and the synchrotron self-absorption frequency ν_a), which in turn depends on the values of the microphysical parameters (the kinetic energy of the outflow E_k, the fraction of energy given to the electrons ϵ_e, the fraction of energy given to the magnetic field ϵ_B, the structure and density of the external medium, and the electron energy index p).

The behaviour of the afterglow light curve is also dependent on whether or not the observer is seeing all of the emission from the jet, which has an opening angle θ. Initially, the radiation contained within the jet will move at a bulk Lorentz factor Γ and will be beamed into an opening angle Γ^{-1}, which is smaller than the jet opening angle, θ. As Γ decreases, the observer will begin to see more and more of the jet until they see the emission from the entire jet at $\Gamma \sim \theta^{-1}$ [49,50]. At this point, an achromatic break in the light curve will occur, known as the 'jet break', after which the light curves will decay at a much steeper rate [49,51,52].

Prior to the launch of *Swift*, the number of GRBs with optical/IR detections was small, around 60 GRBs had optical/IR detections, and only a handful of these had well-sampled optical/IR light curves [53]. The optical/UV behaviour was consistent with power-law behaviour, often with a break in the light curve. The average power-law indices of optical/IR afterglows with observed breaks in their light curves were $\alpha_1 = 1.05 \pm 0.1$ and $\alpha_2 = 2.12 \pm 0.14$ [53]. The first decay index is consistent with the predictions of the closure relations for an isotropic outflow, while the latter decay index is consistent with the decay expected after a jet break. Observations of the optical emission typically began a significant amount of time after the gamma-ray detection, commencing typically more than 0.1 days after the trigger [53]. This left a significant gap in our knowledge of the early optical/IR emission, between the onset of the GRB through to the first few thousand seconds after the trigger. There were also questions as to why not all GRBs had bright optical or radio afterglows, while X-ray afterglows were expected for all GRBs [17]. It was thought that these GRBs were 'dark', potentially due either to dust extinction [54], being (intrinsically) faint and thus not detected when observations occurred several hours after the trigger [55,56], that the optical decayed more rapidly than the X-ray [57], or that they were at high redshift [17]. Prompt high-quality X-ray, UV, and optical observations over the first minutes to hours of the afterglow were thus crucial to obtain a better understanding of GRBs.

3. The Era of *Swifit*/UVOT

Swift, launched in November 2004, has been in successful operation for 18 years. *Swift* was designed specifically to detect GRBs, and observe rapidly with its narrow field instruments. *Swift* houses three instruments that are designed to capture gamma-ray, X-ray, and optical/UV emissions. The Burst Alert Telescope (BAT [58]) detects the prompt gamma-ray emission, while the narrow field instruments, the X-ray Telescope (XRT [59]), and the Ultra-violet/Optical Telescope (UVOT [60]), observe the X-ray and optical/UV afterglow, respectively. The co-alignment of the XRT and *Swift*/UVOT instruments is ideal for observing GRB afterglows because it allows the X-ray and optical/UV emission to be observed simultaneously. *Swift*'s capacity to slew rapidly to point the narrow field of view telescopes at the GRB location, enables regular and early observations of GRBs at longer wavelengths, starting as early as a few tens of seconds after a BAT trigger.

3.1. An Overview of Long GRBs Observed with Swift/UVOT

At the time of writing *Swift*/UVOT has observed ∼1339 long GRBs (https://swift.gsfc.nasa.gov/archive/grb_table/; accessed on 20 October 2022) with $T_{90} > 2$ s. The

majority of GRBs observed by *Swift*/UVOT were initially detected by *Swift*/BAT, resulting in *Swift* automatically slewing to point the *Swift*/XRT and *Swift*/UVOT instruments at the GRB location to rapidly commence observations in the X-ray and optical/UV. However, for a small number of GRBs, *Swift*/UVOT began observations much later, since the gamma-ray emission did not trigger *Swift*/BAT, but was detected either through BAT ground analysis, or by other X-ray/gamma-ray observatories, including the High Energy Transient Explorer-2 (HETE2), the INTErnational Gamma-Ray Astrophysics Laboratory (INTEGRAL), Konus-Wind, the Interplanetary Network (IPN), Fermi, Astro-rivelatore Gamma a Immagini Leggero (AGILE), and MAXI and CALET.

After an automatic slew, *Swift*/UVOT takes its first exposure. This short, typically 10 s, *v* band exposure is taken while the reaction wheels are stabilising *Swift*, such that the pointing direction is in transition from a motion of many arcseconds per second to a stable pointing. During the slew, *Swift*/UVOT is protected from damage by bright stars passing through the field of view by maintaining the photocathode at a low-voltage state. As such, the settling exposure is frequently ignored or discarded [61], since the photometry may be uncertain due to the *Swift*/UVOT photocathode voltage changing at the beginning of the exposure, or concerns regarding the rapidly changing spacecraft attitude [62]. Ref. [63] examined the settling exposure for 26 GRBs detected by *Swift*/UVOT. They found an issue in only 2 out of the 26 GRBs, and only in the first second of the settling exposures. Fortunately, the settling exposure is taken in event mode (in event mode, the arrival times and positions of the individual photons are recorded) and therefore, when issues arise, it does not have to be discarded completely, because it can be cut to exclude the affected parts of the exposure. The settling exposure usually begins 10–15 s before the first settled exposure. The fastest time to settled observations commencing for a long GRB is 52 s after the BAT trigger for GRB 050509A, and the average time to the start of settled observations is 120 s (calculated using GRBs observed by *Swift*/UVOT within the first 500 s, observed as a result of an automatic slew).

Of the ∼1339 long GRBs observed by *Swift*/UVOT, 514 have a reported *Swift*/UVOT detection in at least one *Swift*/UVOT filter (the *Swift*/UVOT filters are *white*, *v*, *b*, *u*, *uvw*1, *uvm*2, and *uvw*2 [60,64,65]); 415 are within the first 500 s after the BAT trigger. This equates to a detection rate of 42% if observed within the first 500 s. This value is consistent with that determined from the second *Swift*/UVOT catalogue, which, when using a sample of 538 GRBs, reported a detection rate of 43% (with a detection threshold of at least 3σ) for long GRBs observed within the first 500 s [62]. If considering a detection threshold of 2σ, rather than 3σ, the detection rate increases to 64% [62]. This is in contrast to 80–90% of GRBs having optical/IR detections observed by ground-based telescopes [66,67]. Examining the number of GRBs with a photometric or spectroscopic redshift, 477 GRBs (36%) observed by *Swift*/UVOT have redshifts (these GRBs may or may not have been detected by *Swift*/UVOT); of these, 289 (22%) have at least one detection in *Swift*/UVOT. The redshift distribution for *Swift*/UVOT GRBs is given in Figure 1. The average redshift for the *Swift*/UVOT observed GRBs is 2.0, while for the *Swift*/UVOT detected GRBs, the average redshift is 1.7. Figure 2 displays the total number of GRBs observed by *Swift*/UVOT per year, together with the number of GRBs observed by *Swift*/UVOT with a measured redshift per year, and the number detected by *Swift*/UVOT with a measured redshift per year. The second panel also provides the fraction of GRBs observed by *Swift*/UVOT with redshift and the fraction of GRBs detected by *Swift*/UVOT with redshift. It is concerning that the number of GRBs observed with *Swift*/UVOT with a reported redshift has decreased over the last 5–10 years, the fraction of GRBs observed with redshift in the first 5 full years of operation (2005–2009) is 47%, while in the last 5 years of operation (2017–2021), this has reduced to 23%. However, while the number of GRBs detected by *Swift*/UVOT with redshift shows a similar decreasing trend, the reduction is not as large, changing from 25% in the first 5 years to 18% in the last 5 years.

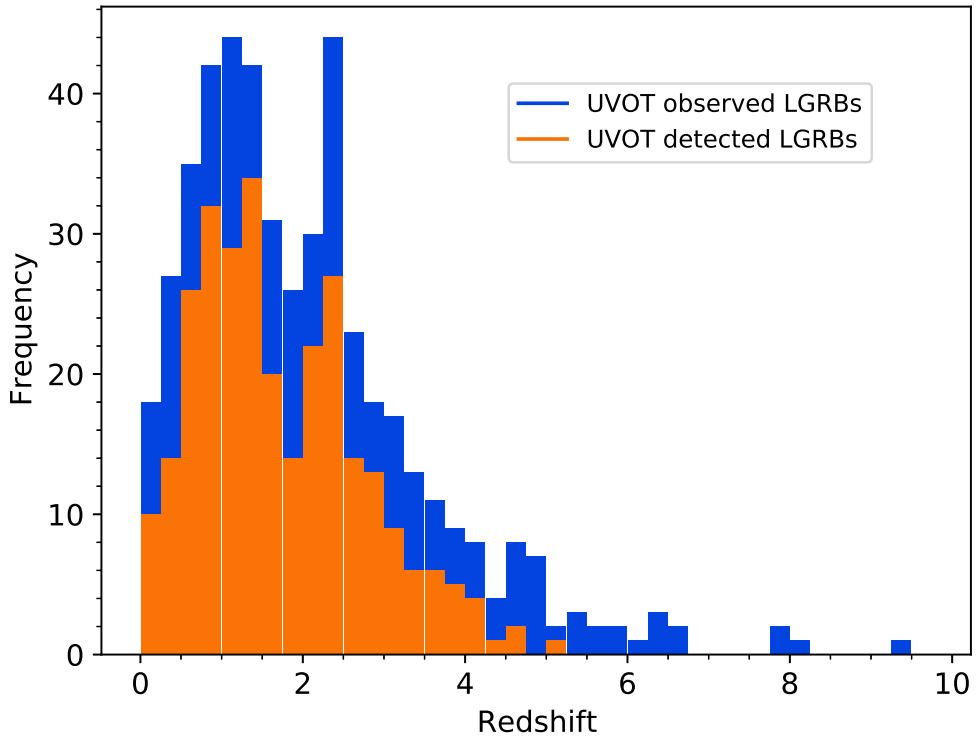

Figure 1. The redshift distribution of *Swift*/UVOT GRBs. The redshift distribution of long GRBs observed by *Swift*/UVOT is given in blue, while the redshift distribution of long GRBs detected by *Swift*/UVOT is given in orange.

In addition to the six lenticular optical/UV filters, *Swift*/UVOT's filter wheel also contains two grisms. These provide low-resolution field spectroscopy in the ultraviolet and optical bands. The UV grism covers the range λ1700–5000 Å with a spectral resolution ($\lambda/\Delta\lambda$) of 75 at λ2600 Å for the source magnitudes of u = 10–16 mag, while the visible grism covers the range λ 2850–6600 Å with a spectral resolution of 100 at λ4000 Å for source magnitudes of b = 12–17 mag [68]. Since November 2008, the automated response sequence of the *Swift*/UVOT, which governs the early exposures after a BAT trigger [60], includes a 50 s UV grism exposure, provided that the burst is bright enough in the gamma-rays. So far, this has resulted in two well-exposed UV spectra for GRB afterglows: GRB 081203A [69] and GRB 130427A [70]. The light curve and grism spectrum for GRB 081203A is given in Figure 3. *Swift*/UVOT has also been able to increase the number of GRBs with known redshift by obtaining photometric redshifts through the analysis of spectral energy distributions built using XRT and *Swift*/UVOT observations of the afterglow, supplemented by ground-based photometry (where available) [61,71–73].

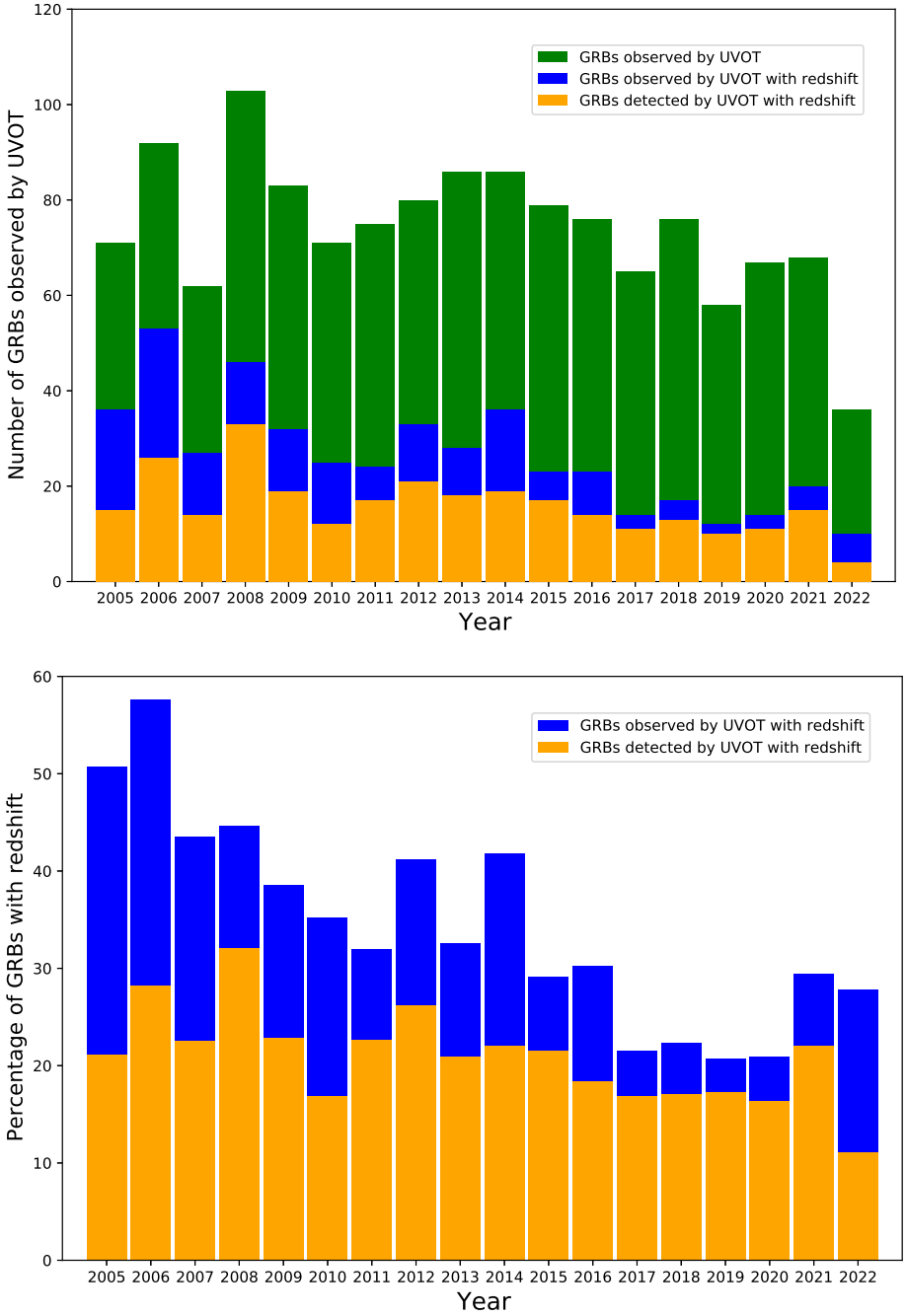

Figure 2. The number of long GRBs observed each year by *Swift*/UVOT. The top panel shows the number of GRBs, while the bottom panel shows the percentage. The green distribution provides the total number of long GRBs observed by *Swift*/UVOT per year. The blue distribution provides the total number/fraction of long GRBs observed by *Swift*/UVOT, which also have redshift, and the green distribution shows the total number/fraction of long GRBs detected by *Swift*/UVOT, which also have redshift. The fraction of long GRBs with redshift and observed by *Swift*/UVOT has steadily decreased with time; however, the fraction of long GRBs with redshift and that have a *Swift*/UVOT detection has not had such a significant reduction.

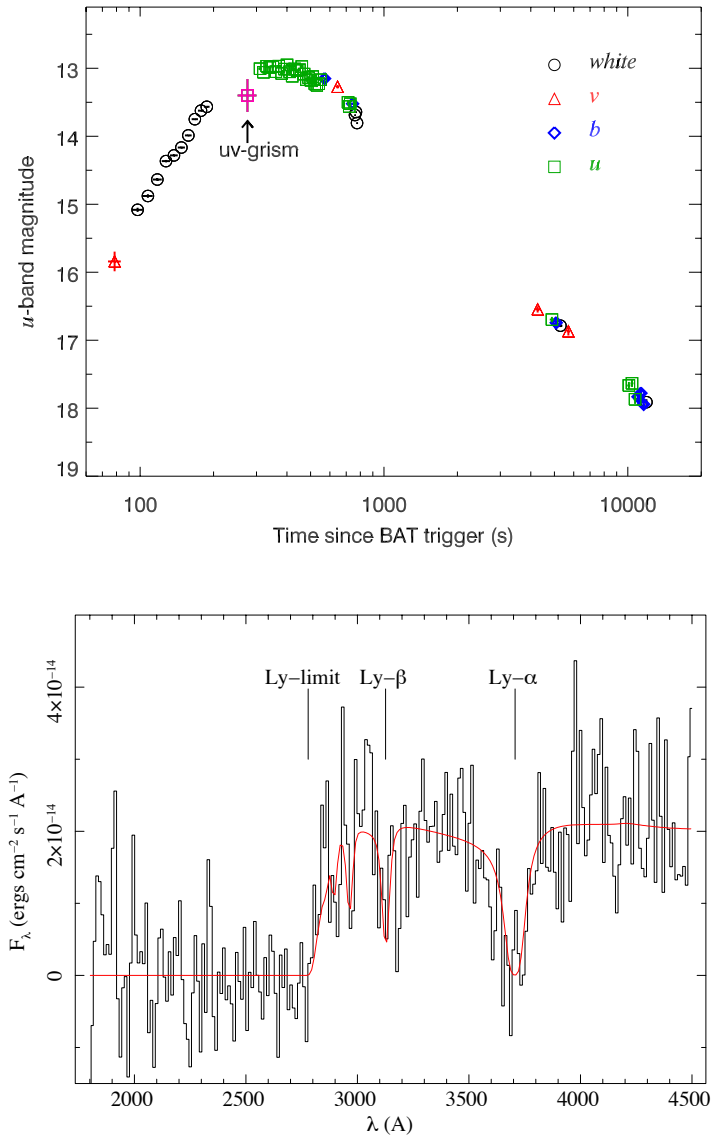

Figure 3. *Swift*/UVOT observations of GRB 081203A (Figures are reproduced from [69], corresponding to Figures 1 and 3 in their article). The top panel displays the optical/UV *Swift*/UVOT light curve of GRB 081203A, including the photometric point derived from the *Swift*/UVOT UV-grism spectrum. The bottom panel displays the UV-grism spectrum of GRB 081203A. The red line is the best-fit model, which includes absorption by Lyman-α, Lyman-β, and the Lyman forest. With these spectral features, a redshift of 2.05 ± 0.01 is derived for this GRB [69].

4. *Swift*/UVOT Long GRB Discoveries

GRB 050318 was the very first GRB to be detected by *Swift*/UVOT [74]. Observations began 3200 s after the BAT trigger, with an initial detection in the v band of 17.8 mag. The optical emission was observed to decay, and the derived spectral and temporal indices were consistent with the expectations of the standard afterglow model, with the fireball expanding into a constant density medium, and the synchrotron cooling frequency lying in between the optical and X-ray bands.

Since GRB 050318, we now have over 1300 GRBs observed with *Swift*/UVOT, and over 500 with a detection by *Swift*/UVOT. Importantly, *Swift*/UVOT has provided a view of the first minutes to hours after the detection of the gamma-ray emission, which was lacking prior to *Swift*, and which provided large numbers of GRBs with simultaneous X-ray and optical/UV observations. While the standard afterglow model, as described in

Section 2.2, has been shown to be a good basic representation of the afterglow emission of *Swift* GRBs, post-*Swift* observations of GRBs often require a more complex model, for instance, with additional emission components or complex jet geometry, which I discuss further in this section. Many advances in GRB science have been through the analysis of multi-wavelength observations, and so, simultaneous observations with *Swift*/UVOT and *Swift*/XRT have been key in unravelling the temporal and spectral behaviour of GRBs. In the rest of this review, I will focus on the most significant advances in GRB science as a result of *Swift*/UVOT's 18 years of operation. I will discuss the most momentous GRBs observed, which due to their brightness, are the best-sampled and best-studied events. I will also discuss rare and usual GRBs observed by *Swift*, and improvements to our understanding of dark GRBs, the morphology of optical/UV light curves and correlations discovered with optical/UV observations.

4.1. Record-Breaking GRBs

The detection of GRB 050318 was just the start of many major discoveries by *Swift* and *Swift*/UVOT. Over the years, *Swift* has detected several GRBs that have pushed the boundaries of our expectations and knowledge. Some of the most striking and informative are the brightest GRBs observed via UVOT. These GRBs have the best signal-to-noise *Swift*/UVOT light curves, and they are events that tend to be intensely observed by a whole range of ground- and space-based facilities. Every few years, *Swift* delights us with an even more remarkable example. These events tend to be bright, due to a combination of being intrinsically bright (isotropic gamma-ray energy, E_{iso}, $\sim 10^{54}$ erg) and relatively nearby ($z \lesssim 1$), compared to the typical redshift of *Swift*/UVOT-detected GRBs (see Figure 1).

The first markedly bright GRB was GRB 061007. At the time, it was the brightest observed by *Swift*/UVOT, and one of the brightest to be detected by *Swift* in BAT and XRT [75,76]. This GRB was at a redshift of 1.26 [77] and had an $E_{iso} \sim 1 \times 10^{54}$ erg [78]. The afterglow had a v-band magnitude <11.1 at 80 s, after the prompt emission [75]. This GRB was surpassed in brightness, a couple of years later, with the detection of GRB 080319B. This GRB was at a redshift of 0.937 [79] and had a V-band magnitude of 5.3 during the prompt emission. It was dubbed the 'naked eye GRB' as it would have been visible to the naked eye for a few tens of seconds for an observer in a dark location looking at the right time and place. GRB 080319B saturated the *Swift*/UVOT *white* filter for the first $\sim$970 s after the BAT trigger. From $\sim$ 280s, a measurement could, however, be achieved in the v filter. For this GRB afterglow, a two-component afterglow model was necessary to explain the complex behaviour of the optical-X-ray emission [80]. The previous record holder for optical brightness was a pre-*Swift* GRB, GRB 990123, with a ninth magnitude V-band observation.

GRB 1304027A was a v=12th mag, luminous ($E_{iso} \sim 8 \times 10^{53}$ erg; [70]) and unusually close by ($z = 0.34$; [81]) GRB. Such a nearby and luminous event was predicted to occur once every 60 years [70]. Long GRBs at $z < 0.4$ tend to be sub-luminous ($E_{iso} < 10^{52}$ erg, see also Section 4.2), and so GRB 130427A was unusual in that its behaviour is more consistent with GRB occurring at $z \sim 1$–2. It was thus given the moniker 'a nearby ordinary monster' [70]. GRB 160625B was another bright GRB. It triggered Fermi [82,83], but unfortunately not *Swift*/BAT, and so the early optical behaviour was missed by *Swift*/UVOT. Observations only began with *Swift*/UVOT 9ks after the Fermi trigger [27]. GRB 190114C had similar redshift and isotropic energy as GRB 130427A [84]; it had a bright, 13th mag optical/UV afterglow, and was the first GRB to have TeV photons reported and detected in the range of 0.2–1 TeV [85].

The latest addition to this collection of bright events observed by *Swift*/UVOT is the very recently detected GRB 221009A [86,87]. This GRB was initially thought to be an X-ray transient due to its unusual gamma-ray behaviour observed by *Swift*/BAT, and its apparent location within the Galactic plane. However, its status as a GRB was confirmed with the X-ray light curve decaying as expected for a GRB afterglow [87], and subsequently, a redshift determination of 0.151 [88–90]. Most unusually, many facilities, including Fermi,

AGILE, Konus-Wind, and INTEGRAL, reported detecting X-ray and gamma-ray emission from this GRB an hour prior to the *Swift* detection [91–98]. It is also the second GRB to be detected at TeV energies, and the first with photons of above 10 TeV [99], with one photon being reported at 251 TeV [100]. The isotropic energy from this event is still to be confirmed, but initial estimates suggest it is $E_{iso} \sim 1$–6×10^{54} [94,96,101,102], close to that of GRB 160625B [101]. Since *Swift*/BAT triggered on the afterglow emission (the first time in 18 years) rather than the prompt gamma-ray emission, *Swift*/UVOT observations only began an hour after the Fermi trigger [103]. In addition, due to the GRB's closeness to the Galactic plane, the optical/UV emission is affected by significant galactic extinction ($A_v \simeq 4$ mag increasing in the UV to an $A_{uvw2} \simeq 10$ mag). Given these restrictions, GRB 221009A was still detected in the initial *Swift*/UVOT v image at 16.6 mag, and marginally detected in $uvw1$. Such a nearby and bright event is only expected once in 1000 years [103]. The results of the detailed analysis of this GRB are starting to be published; see [27,90,102–140]. The *Swift*/UVOT light curves of all these bright GRBs are given in Figure 4.

4.2. Rare and Unusual GRBs

As well as spectacular GRBs in terms of optical brightness, *Swift*/UVOT has observed GRBs with rare and unexpected behaviour. Prior to *Swift*, the nearest GRBs to us were GRB 980425 [141,142] at $z = 0.0085$, followed by GRB 031203A at 0.105 [143,144], and GRB 030329 at z = 0.168 [145,146]. GRB 980425 and GRB 031203 were of low luminosity, atypical of the bulk of cosmological GRBs. *Swift* has increased the number of detected rare and nearby long GRBs, with GRB 060218 at z=0.033 [147], GRB 100316D at z = 0.0591 [148], and GRB 111005A at z = 0.01326 [149,150]. These GRBs were also of low luminosity, and along with GRB 980425 and GRB 031203, they are categorised as low-luminosity GRBs (LLGRBs). All of these events, except GRB 111005A [149,150], are associated with a type Ib/c supernova, supporting the connection between GRBs and the collapse of massive stars. Unfortunately, GRB 111005A was constrained by the Sun and thus was not observable with *Swift*/UVOT, and no variable optical or UV source was detected for GRB 100316D, which was hampered by the bright underlying host galaxy [148]. However, *Swift*/UVOT did detect optical/UV emission from GRB 060218, with observations starting ∼100 s after the gamma-ray trigger. In this case, *Swift*/UVOT observations were important to constrain a thermal component, found initially in the X-ray spectrum, as it cooled and shifted with time into the optical/UV [151–153]. This was suggested to be the 'shock break out' of the supernova, the moment where the shock wave breaks out of the star [151,152]. This was the first time such an observation was observed with a GRB.

Over the years, a small number of GRBs have been found by *Swift* and other gamma-ray detectors to have $T_{90} > 1000$ s [154–156], including GRB 060218 and GRB 100316D. An even smaller number are ultra-long GRBs (ULGRBs), with $T_{90} > 2000$ s [154,155]. Of these, *Swift* detected: GRB 101225A at $z = 0.847$ [155,157,158], GRB 111209A at $z = 0.677$ [154,156,159,160], GRB 121027A at $z = 1.773$ [155], and GRB 130925A at $z = 0.347$ [161–163] (other candidate ULGRBs are discussed in [156]). While all four were observed by *Swift*/UVOT, only GRB 101225A and GRB 111209A have well-sampled *Swift*/UVOT light curves. GRB 130925A was not detected by *Swift*/UVOT, and GRB 121027A was only weakly detected in $white$, which may be due to its larger distance compared to GRB 101225A and GRB 111209A [155,164]. The main difficulty in determining the nature of ULGRBs is in explaining their long gamma-ray duration. It has been suggested that they are caused by the collapse of massive stars with radii that are larger than that considered for typical GRB progenitors [154,155]. An alternative suggestion is that these are the tidal disruption of white dwarfs as they pass close to a supermassive black hole (SMBH), for which the black hole is at the lower mass end of the SMBH distribution (e.g., $<10^5 M_\odot$) [155]. An analysis of the *Swift*/UVOT and GROND data of GRB 111209A by [156] suggests that the optical/UV afterglow is consistent with the main population of long GRBs in terms of its luminosity distribution. They also state that while GRB 111209A has an isotropic energy and peak energy at the high end of the GRB distribution in terms of prompt emission parameters, these parameters are consistent with the

Amati and Ghirlanda relations [165,166], suggesting that this and potentially other ULGRBs may not be a distinct class. Ref. [156] also notes that GRB 101225A is more unusual in its optical/UV behaviour compared to the other ULGRBs, and may have a distinctive progenitor. GRB 101225A has been explained by [157] as an inspiral of a neutron star into a helium star, creating a central engine similar to a GRB.

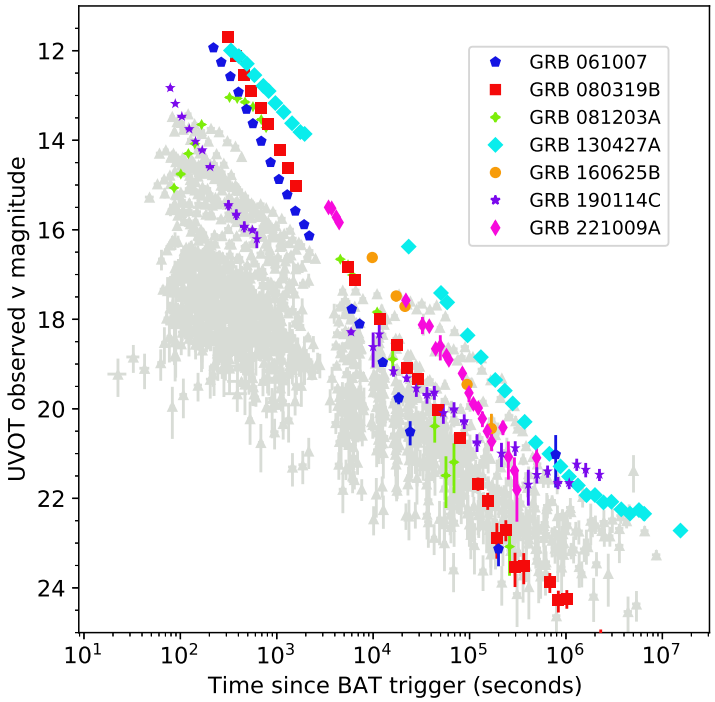

Figure 4. A sample of long GRB UVOT light curves. Those in colour are the brightest observed by UVOT (see Section 4.1) and include GRB 061007, GRB 080319B, GRB 081203A, GRB 160625B, GRB 190114C, and GRB 221009A. The grey light curves are UVOT-observed GRBs discovered between 2005 and 2010, taken from [61]. To create each light curve, individual colour filters (*b*, *u*, *uvw*1, *uvm*2, *uvw*2, and *white*) were normalised to the *v*-band light curve and were co-added to construct a single filter, *v*-band, and light curve. These light curves have not been corrected for extinction. For the light curves highlighted in colour, the extinction is small $A_v < 0.5$ mag, except for GRB 221009A, which has a significant extinction with $A_v = 4.1$ mag [167].

4.3. Dark GRBs

Before moving on to discuss what we have learned about the optical/UV behaviour of GRBs, it is important to discuss the large fraction of long GRBs that were observed by *Swift*/UVOT but not detected, ∼40–60%, depending on the detection threshold (see Section 3.1). The optical/UV afterglows of some GRBs may not be detected due to observational constraints such as the rapidity of telescope pointing; and the GRB location relative to the Sun, Moon, and other bright sources. Restricting the sample to those observed by *Swift*/UVOT within the first 500 s after the gamma-ray detection and without observing constraints, there is still a significant fraction that are 'dark'. Formally, GRBs are considered to be "dark" if their X-ray to optical spectral index is $\beta_{OX} < \beta_X - 0.5$ [168], and so, some GRBs may be considered to be 'dark', even with the detection of the optical/IR emission. The percentage of 'dark' GRBs typically found for different instruments is 20–50% [66,67,169,170]. With the rapid slewing capabilities of *Swift*, observations with *Swift*/UVOT have enabled us to rule out these dark GRBs as being due to factors such as a lack of sensitivity, late observation times, and rapid temporal decays [171]. The low detection rate or "darkness", could however, be due to one or more of the following: a high background due to a small Sun-to-field angle [172], a large galactic extinction (e.g., [172,173]), a high circumburst extinction (e.g., [174–176]), intrinsic faintness [175], and Lyα damping due to high redshift

(e.g., [57,174,175,177]). Several studies, including those using *Swift*/UVOT observations (e.g., [72]), have suggested that high circumburst extinction and high-redshift are the two main causes for why GRBs are 'dark' [67,170,171,178].

4.4. The Optical/UV Behaviour of Swift/UVOT Observed GRBs

Swift/UVOT has provided the GRB community with the largest sample of optical/UV observations of GRBs to date, with observations beginning typically 120 s after the detection of the gamma-ray emission. We now have a good idea of how GRBs behave in the optical/UV range from the first few minutes after detection, through to the first few days, beyond which they typically fade below the detection sensitivity of *Swift*/UVOT.

Since X-ray and optical/UV observations are taken simultaneously, it is useful to compare the temporal behaviour in both bands. Not long after the launch of *Swift*, the X-ray light curves were shown to have two unexpected features: an initial steep decay, thought to be due to the tail of the prompt emission, and a shallow decline phase whose nature is not yet resolved, but may be due to a long lived central engine [179] or a short lived central engine that emitted shells over a wide range of velocities, with the slower shells catching up at a later time to continuously eject energy into the ejecta [180]. These two power-law segments, in addition to the two power-law segments observed pre-*Swift*, the normal decay and the post-jet break decay, lead to the creation of a 'canonical' X-ray light curve, whereby most X-ray light curves can be fitted with one or more of these power-law decays, and X-ray flares may also be additionally superimposed [181,182].

In the optical/UV, it was shown that the optical/UV light curves behave more simply [183], with an initial study of optical/UV light curves observed by *Swift*/UVOT, showing that the light curves decay as a simple or broken power-law, and with a small number displaying an initial rise to a peak before they decay. Later, with a larger sample of GRBs, the optical/UV light curves could be grouped into different morphologies [62] in a similar fashion, as was achieved for the X-ray light curves [184]. The morphologies are shown in the eight panels of Figure 5, (a) a 'canonical' light curve, (b) a break to a shallower decline, (c) a break to a steeper decline, (d) no break, (e) a gentle rise, transitioning to a steep decay, followed by a shallow decay, then another steep decay, and finally a more gentle decay; (f) starts with a rapid, steep decay, then a rise to peak (in some instances, with a break within the rise), a steep decay, and a final less-steep decay. Panels (a–d) are the same as those used for the X-ray light curves, while (e) and (f) are specific to the optical/UV emission. The final shallow decay in (f) is likely a result of poor background subtraction due to the background host signal dominating over the GRB signal. Using this scheme, approximately half of the optical/UV afterglows observed by *Swift*/UVOT are consistent with panel (d), a simple power-law, 21% are consistent in behaviour with the scheme in panel (e), with a few percent being consistent with each of the other panels. In comparison for the X-ray light curves, 42% are consistent with panel (a) canonical, 30% are consistent with one break, 15% with panel (b) and 15% with panel (c), 4% are consistent with panel (d) a simple power-law, and a further 24% are considered to be oddballs, displaying a range of behaviour that is not consistent with these specific types. This morphological categorisation provides some indication of the number and frequency of emission components producing the X-ray and optical light curves. For the optical/UV, at least ∼50% are consistent with panel d), which suggests that typically, a single emission component is sufficient to produce all of the optical/UV emission. For the X-ray light curves, the largest fraction of GRBs are consistent with panel (a), suggesting a more complex scenario with multiple emission components producing the X-ray emission, as described in the previous paragraph. However, ref. [62] states that poorly sampled light curves tend to be consistent with a power-law, and so light curves with poor sampling may have more complex behaviour than that observed.

The range in optical/UV behaviour can also be displayed as a canonical optical light curve [185] in a similar way as was done for the X-ray canonical light curve [181,182], with the optical/UV afterglow comprised of or more components: prompt optical flares, an early optical flare from the reverse shock, shallow-decay segment, the standard afterglow

component (an onset hump followed by a normal decay segment), the post-jet-break phase, optical flares, rebrightening humps, and late supernova bumps [185]. I will now focus on the particular features observed in the optical/UV light curves.

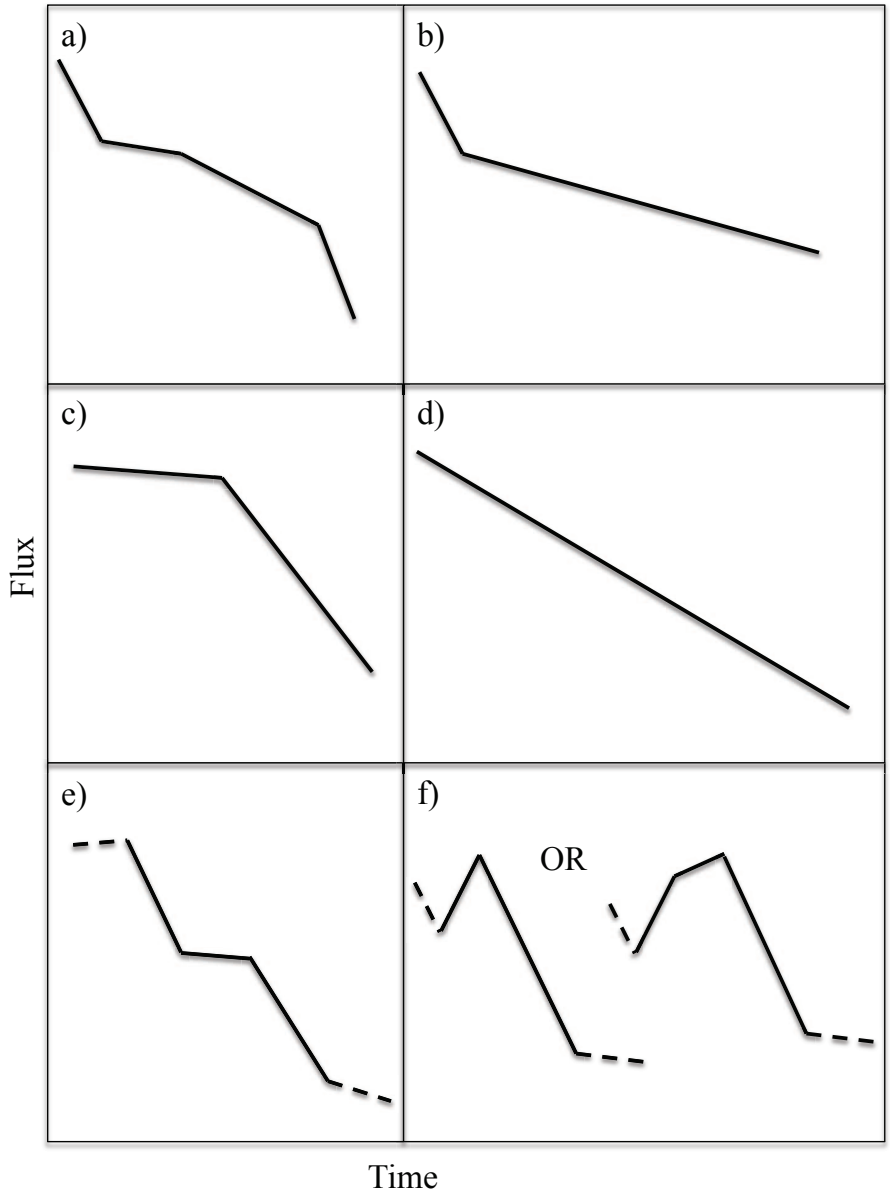

Figure 5. Schematics of GRB optical/UV light-curve morphologies, as derived from [62]. Morphologies (**a**–**d**) are the same as those used to describe the X-ray light curves in [184], but morphologies (**e**–**f**) are specific to the optical/UV. These additional two morphologies represent 25% of the *Swift*/UVOT GRB light curves. Dotted lines represent those portions of the light curves that are not always seen in these morphologies. The percentage of *Swift*/UVOT light curves corresponding to the different panels are: (**a**) 7%, (**b**) 7%, (**c**) 14%, (**d**) 47%, (**e**) 21%, and (**f**) 4%. This figure is reproduced from Figure 4 of [62]. ©AAS. Reproduced with permission.

4.4.1. Early Optical Emission

Some of the most informative and important observations *Swift*/UVOT has performed have been in relation to the earliest phases of the optical/UV GRB emission, within the first few hundred seconds. Optical/UV emission, when detected, is observed from the earliest moment that *Swift*/UVOT observations begin [63]. In the majority of cases, the optical/UV emission is already declining by the time *Swift*/UVOT observations begin, and only around

20% are observed to have an initial rise to a peak in their light curves [62,63,183]. A correlation has been observed by [186–188] between the peak time and the peak brightness of optical afterglows, but for the majority of GRBs, we do not have a measure for either parameter. Since all of the optical/UV light curves must rise initially, this suggests the need for an even faster response to catch the start of the optical/UV emission.

There are two possible origins for the early optical/UV emission. It could either be produced by the external shocks that are generated as the ejecta are slowed by the external medium, or the optical emission could be related to prompt gamma-ray emission, which in turn is thought to be produced internally to the outflow. The observed emission may also be a combination of both possibilities, with different components dominating at different times for different GRBs. For the majority of GRBs, the prompt emission is not thought to be the dominant emission mechanism producing the early optical/UV emission of *Swift*/UVOT observed GRBs, but it is observed in some [63,189]. Examples where the prompt emission contributes to the early optical/UV emission observed by *Swift*/UVOT are GRB 061121 [190,191], GRB 080928 [191,192], GRB 110205A [191], and the ULGRB GRB 111209A [156,160]. In addition, prompt emission produced some of the very early optical emission of GRB 080319B [80], before *Swift*/UVOT began observations. Simultaneous observations of the prompt emission across multiple wavelengths are rare but important for understanding the origin of the prompt emission and the transition to the afterglow phase [191].

For the small fraction of GRBs with early observed rises in their optical/UV light curves, there are a number of mechanisms that may produce it. In some cases, an initial rise may be due to the prompt emission [189]. Observed rises may also be produced by the external shock. Both the forward and reverse shocks could produce a rise in the optical/UV afterglow, and may even be a combination of both [193–196]; see Figure 6. In the forward shock, a rise may be produced as a result of the jet slowing down as it ploughs into the external medium (the onset of the afterglow) or the passage of ν_m through the optical bandpass [52,193]. If the rise is due to the start of the forward shock, it should also be observed in the X-rays, but it is generally masked by the tail of the prompt emission [197,198]. In a sample of *Swift*/UVOT optical/UV light curves with observed initial rises, the passage of ν_m could be excluded as the cause of the initial peak, and there was no evidence for reverse shock emission [183]. The rise in these optical/UV light curves and other early optical light curves samples suggested that the rise could be attributed to the start of the forward shock [183,199,200]. More recent work [196], with a larger sample of GRBs suggests that optical rises are produced by all possible combinations of forward and reverse shocks, as shown in Figure 6, with $\sim$ 50% of rises being consistent with the start of the forward shock (bottom left of Figure 6). The least common type of rise was initially dominated by the reverse shock that quickly fades, and then a second peak occurs due to the passage of ν_m through the optical band of the forward shock [196]. It is possible, however, that some of these optical rises occur while the prompt emission is still active, and so they could also be explained as internal origin [189].

For optical rises produced by the onset of the afterglow, the peak time of the optical light curve depends on whether the shell that collides with the surrounding interstellar medium is thick or thin. For thick shells, the peak time, t_{peak}, of the optical emission will be comparable to T_{90} [201,202]. In the thin shell case, the optical peak is expected after T_{90} [199,200]. Providing that the peak occurs when $t_{peak} > T_{90}$ (thin shell regime), then the Lorentz factor of the shell at the moment of the peak, Γ_{peak}, can be derived [1,52,199]; Γ_{peak} is expected to be half of the initial value Γ_0 [203,204]. A lower limit can be obtained for those GRBs where the peak occurs before the onset of observations (>100; [183]). For GRBs with observed rises, Γ_0 ranges from 100 to 1000 [183,186,199,200], consistent with expectations that Γ_0 must be at least 100 in order to produce gamma-ray emissions [205,206]. Using Γ_{peak}, it is possible to deduce two more quantities: the isotropic-equivalent mass of the baryonic load, M_{fb}, and the deceleration radius, R_{dec} [199]. The deceleration radius defines the radius, in a thin shell regime, at which the accumulated external medium is $1/\Gamma_0$ of the

ejecta mass. The mean mass of the baryonic load and the mean deceleration radius for GRBs with an observed rise is $\langle M_{fb} \rangle \sim 4 \times 10^{-3}\,\mathrm{M}_{\odot}$ and $\langle R_{dec} \rangle \sim 2 \times 10^{17}$ cm. For GRBs without observed rises, the quantities are $\langle M_{fb} \rangle \lesssim 1 \times 10^{-3}\,\mathrm{M}_{\odot}$ and $\langle R_{dec} \rangle \lesssim 1 \times 10^{17}$ cm [183,186]. These deceleration radii are consistent with the value expected from the forward shock model, $R_{dec} \sim 10^{16}$ cm [207]. The internal shocks, that are believed to power the prompt emission, are expected to occur at $\sim 10^{15}$ cm [208,209].

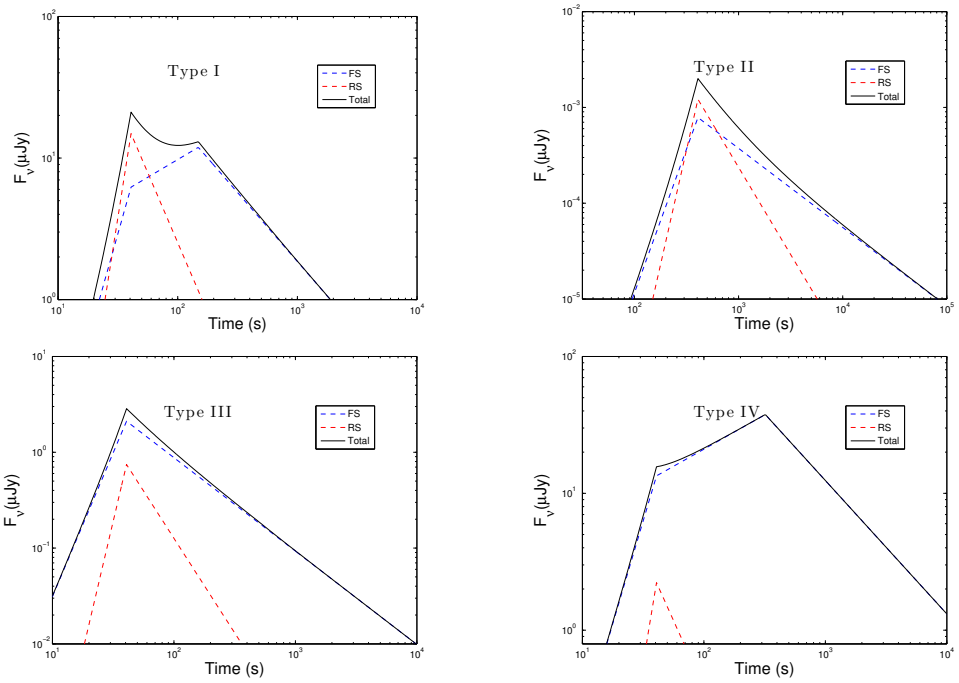

Figure 6. Example optical light curves for four different scenarios of early afterglow behaviour resulting from the combination of forward and reverse shock emission [196]. Top left panel (**type 1**): the light curve is initially dominated by the reverse shock (RS) emission, but the reverse shock quickly fades and a second peak is produced as ν_m crosses the optical band in the forward shock (FS). Top right (**type II**): the forward shock and reverse shock peak at the same time, but the reverse shock dominates the emission at the peak. The reverse shock quickly fades and the decaying forward shock emission dominates at late times. Bottom left (**type III**): the forward shock always dominates; the reverse shock is weak or suppressed. The peak is due to the onset of the forward shock emission. Bottom right (**type IV**): the forward shock dominates, and the reverse shock is weak or suppressed. The onset of the forward shock emission produces the first (lower) peak; the main peak occurs when ν_m crosses the optical band. Figures reproduced from Figure 1 of [196]. ©AAS. Reproduced with permission.

4.4.2. Optical Flares

Flares in X-ray light curves had been seen prior to *Swift*, but only a handful of times (e.g., [22,210,211]). With the launch of *Swift*, it was quickly shown that they are quite common [212,213], appearing in approximately 50% of XRT afterglows [214], occurring generally after the end of T_{90}, and were superimposed on the X-ray light curve. These X-ray flares are thought to be due to the same processes that produce the prompt gamma-ray emission [215,216]. Flares are also observed in the optical/UV light curve (see example in Figure 7). However, they are generally not as prominent as those in the X-rays, not as frequent [185], and were likely to be overlooked or dismissed as noise [217].

Using a blind, systematic search for flares, ref. [217] analysed 201 *Swift*/UVOT GRB light curves, and found episodes of flaring in 68 (∼34%); a lower fraction than that found in X-ray light curve samples (50%), but higher than previous optical studies (12% [185]). On average, two flares were found in each of the 68 GRBs with flares. Ref. [217] found that

most of the flares occur within the first 1000 s of the afterglow, but could be observed and detected beyond 10^5 s. More than 80% of the flares detected are short in duration, with $\Delta t/t$ of $<$0.5. Ref. [218] investigated further the *Swift*/UVOT optical flares found by [217]. Ref. [218] found a correlation between the rise and decay times of the optical flares, and a correlation between their duration and peak time. These correlations are consistent with the results of X-ray flares, suggesting they share the same physical origin, and both being possibly produced via internal emission as a result of central engine activity [218].

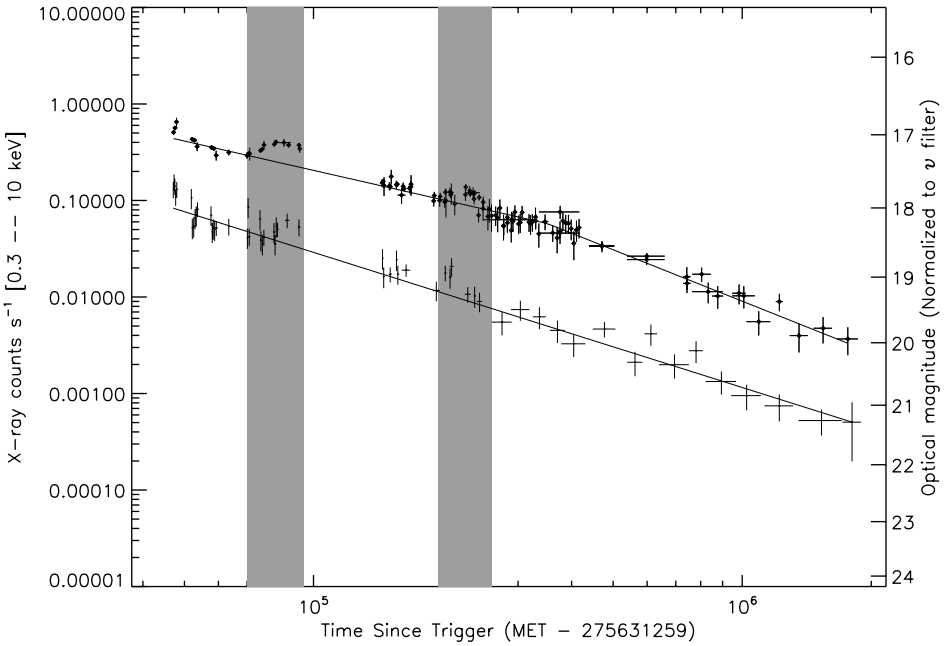

Figure 7. X-ray and optical/UV light curves of GRB 090926A. Flaring periods are shaded in grey. The *Swift*/UVOT light curve is given at the top (circles); the XRT light curve is below (pluses). Figure reproduced from Figure 2 of [219]. ©AAS. Reproduced with permission.

4.4.3. Optical Rebrightenings

Another feature found in the *Swift*/UVOT observations are late optical/UV rebrightening bumps (e.g., GRB 100815A; [220,221]). These have been detected in around 18% of optical light curves [188]. These bumps occur after the initial onset and detection of the optical emission, and they are distinctive from bumps produced by an accompanying supernova. Supernovae occur later, peaking around one to two weeks after a GRB trigger, and they are generally red in colour. While some rebrightening bumps can be explained through a combination of reverse and forward shocks (e.g., the top left panel of Figure 6; [221]), many require a structured jet [188]. In this case, the jet is not a simple uniform jet, but the energy and Lorentz factor of different parts of the jet varies and is dependent on the angle away from the jet axis. The simplest structured jet is a two-component outflow, which has an inner, narrow jet and an outer, wider jet encompassing the narrow jet. The narrow jet produces the prompt emission together with the initial optical emission, and the wider outflow dominates the optical emission at later times [222]. This model interprets the rebrightening bump as the deceleration of the second slow jet. A two-component outflow model has a great deal of flexibility. Variations on this model have been used to explain the behaviours of GRBs with breaks in the X-ray light curves, which are geometric in nature (e.g., no spectral evolution is observed at the time of the X-ray break; spectral evolution would have indicated that the break was due to the passage of a synchrotron frequency through the observing band), but they have no corresponding break in the optical/UV light curves, which would otherwise be expected in the uniform jet model (e.g., [80,223,224]).

4.4.4. Jet Breaks

Jet breaks were thought to be observed in pre-*Swift* observations of GRBs (e.g., [53,225,226]), however, only a few were confirmed as being achromatic [227–229]. While there have been some cases of confirmed achromatic jet breaks in post-*Swift* GRBs (e.g., GRB 050525A and GRB 140629A; [230,231]), they are small in number [184,232–234], and for some GRBs, no jet break has been detected for months [235] or even years after the initial gamma-ray detection [221]. These extreme cases can pose problems for the external shock models, requiring extreme values of the physical parameters of the explosion, the emission mechanism, and the environment to explain them [221]. In general, however, the lack of detected jet breaks for many GRBs may likely be, at least in part, due to the lack of good coverage, particularly in the optical/UV. Of 900 GRBs studied by [236], only 85 had well-sampled optical and X-ray afterglows. Within these 85, ref. [237] found that around half had achromatic breaks, consistent with being a jet break [237], with a wide range of jet break time, from a few hundred seconds, up to 250 ks. When a jet break can be determined, it can be used to constrain the opening angle of the jet, with values found to range from $\sim 1^\circ$ to $\sim 50^\circ$ (e.g., [150,238], see also references therein) and a typical value $\theta_j = (2.5 \pm 1.0)^\circ$ [237]. The jet opening angle can be used to compute the geometrically corrected energy of a GRB as the energy of a GRB is concentrated with a jet and not emitted isotropically. The authors of [237] compute a beaming-corrected gamma-ray energy $\log E_\gamma = (49.54 \pm 1.29)$ erg and a geometrically corrected kinetic energy (E_K), the blastwave kinetic energy is computed from the optical afterglow, $\log E_K = (51.33 \pm 0.58)$ erg. With E_γ and E_K, the radiative efficiency of the jet can be computed [239,240]. Most GRBs in [237] have a small radiative efficiency of $<10\%$ at the time of the jet break. Determining accurate values for the θ_j and E_γ, as well as the time of the jet break, t_{jet}, are important for GRB correlations (e.g., [166,225,241]). The opening angle of the GRB jets, θ_j, is also important in constraining the total GRB event rate density, with ref. [237] finding twice that of pre-*Swift* estimates [225,242].

4.4.5. Afterglow Luminosity and Correlations

Soon after the launch of *Swift*, several works found a bimodal optical luminosity distribution [243–245], implying two populations of optically bright GRBs. However, other studies [66,169,246–248], including one study consisting only of *Swift*/UVOT light curves [183], only required a single population to describe the optical luminosity distribution. A single population seems to best represent the distribution even as the sample continues to increase in size (e.g., [249]).

Studies of single GRBs provide exceptional detail on the behaviour and physical properties of individual events. However, statistical investigations of large samples of GRBs aim to find common characteristics and correlations that link individual events and that therefore provide insight into the mechanisms common to GRBs. Statistical investigations have benefited greatly post-*Swift* launch from the observation of large numbers of GRBs with well-sampled X-ray and optical/UV observations. This has led to a number of correlations being discovered in the *Swift* era within the afterglow emission and linking the prompt gamma-ray emission [241,246,250–252]. This is most notable between the intrinsic afterglow brightness and the isotropic energy of the prompt emission [251,253–257], which suggest the most energetic GRBs in the prompt emission have also the brightest afterglows. Since the isotropic energy of the prompt emission is correlated with the intrinsic prompt emission peak energy [165,258], this also implies a three-parameter correlation between the isotropic energy of the prompt emission, the intrinsic prompt emission peak energy, and the X-ray afterglow brightness [250–252]. The intrinsic brightness of the afterglow in the X-ray and optical light curves are also correlated, such that GRBs with bright X-ray afterglows have also bright optical afterglows [257], see also [259–261]. The Liang–Zhang correlation is another three-parameter correlation between the isotropic energy of the prompt emission, the intrinsic prompt emission peak energy, and the jet break time [241]. For recent reviews describing all GRB correlations in the prompt and afterglow emission, see [262–264] and references therein. For a recent, comprehensive, and systematic study of all GRB parameters

and correlations, see [265]. Three correlations have been discovered using only optical/UV afterglow observations, which I will expand upon below.

Refs. [186,187,266,267] find a significant correlation between the peak time and peak afterglow brightness in both the X-ray and optical light curves of those GRBs with observed rises. Ref. [186] used the peak time to determine the initial Lorentz factor of the outflow, finding it to be correlated with the isotropic gamma-ray energy.

Within samples of optical light curves [185,268,269] a correlation is found between the restframe time at the end of the plateau phase, with the luminosity at the same time (see also [187]). This correlation is also present in the X-ray light curves [270–273], and in GeV light curves [274]. A theoretical interpretation of this correlation is that it may be explained within the context of the standard fireball model through the evolution of the microphysical parameters [275,276]. Alternatively, it may be explained by the spindown of a newly born magnetar [179,250,277–279], or by structured jets viewed over a range of viewing angles [280]. An extension of this optical luminosity-plateau end time correlation (also known as the Dainotti relation) has been obtained by adding the peak prompt luminosity, leading to a three-parameter 'Fundamental Plane' correlation [269], which was also shown to be present in the X-ray light curve sample [281,282].

Using the *Swift*/UVOT optical light curves, [61] discovered a correlation between the early luminosity (at restframe 200 s) and the average rate of decay (measured with a single power-law from 200 s until the end of observations), see Figure 8. This correlation was also shown to be present at X-ray wavelengths [257,283], and most recently, in a small sample of GeV light curves [284]. The early X-ray and optical/UV luminosity also correlates with the isotropic energy of the prompt emission [251,256,257], implying that the most energetic GRBs have the brightest and fastest decaying afterglows [257]. This correlation may be explained via a parameter or mechanism that controls the energy release in GRBs, such that the most energetic GRBs lose their energy quicker, or may be a viewing angle effect, such that GRBs viewed off-axis have fainter and slower decaying light curves [61,222,266]. As this correlation is present in samples of X-ray light curves with and without plateau phases [283], it will be important to determine how the luminosity-plateau end time relation relates to the luminosity-decay rate correlation.

Since the luminosity-decay rate and luminosity-plateau end-time correlations relate intrinsic parameters to observed ones, it is hoped that these and other GRB correlations may be used to standardise GRBs, to determine redshifts for GRBs without a spectroscopic or photometrically measured redshift, and for use as standard candles, as was achieved using the Philips relation [285] for SNe Ia (e.g., [286]). This has so far been implemented for several correlations involving prompt emission parameters (e.g., [262,287–293]), and the X-ray versions of the luminosity-plateau end-time correlation and the three-parameter 'Fundamental Plane' correlation [269,273,279,294–297].

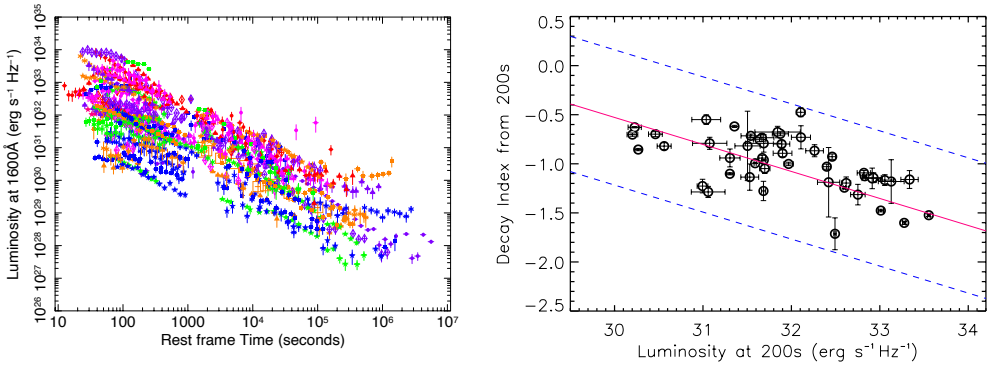

Figure 8. Left: Optical luminosity light curves of 56 GRBs at restframe 1600 Å. Right: Average decay index determined from 48 optical luminosity light curves after 200 s versus luminosity at 200 s. The red solid line represents the best-fit regression, and the blue dashed line represents the 3σ deviation. Figures reproduced from Figures 1 and 2 of [61].

5. Conclusions/Looking to the Future

Swift has been a highly successful GRB mission for the last 18 years and continues to be the workhorse of the GRB and transient community. The flexibility and responsiveness of *Swift*, in part due to its excellent and dedicated team, ensures that *Swift* continues to provide key observations to the astronomical community, and continues to be a successful top-ranked NASA mission.

Swift/UVOT observations have revolutionised our understanding of the optical/UV emission of GRBs, providing information on the behaviour of the optical/UV emission in the first minutes to hours after the gamma-ray emission, which was unknown prior to *Swift*. Over the past 18 years, *Swift*/UVOT has provided large numbers of optical/UV observations of GRBs with simultaneous X-ray observations. *Swift*/UVOT and *Swift*/XRT have highlighted the importance of multi-wavelength observations and analyses, which have been key in unravelling the temporal and spectral behaviour of GRBs. The optical/UV light curves can be more complex than expected pre-*Swift*, with optical flares and optical rebrightenings sometimes being superimposed on the expected standard afterglow emission. This behaviour does not always trace the X-ray light curves, and in some cases, it suggests multiple emission components or that a complex jet structure is needed to explain the observations. In particular, 20% of the early optical light curves are observed initially to rise, which is not observed in the X-ray.

The number of well-sampled optical/UV light curves observed by *Swift*/UVOT has enabled statistical analyses to be performed, resulting in the discovery of correlations between parameters measured from the optical/UV afterglows, and also from the gamma-ray emission, thus connecting to the processes resulting in the prompt and afterglow emission. The optical/UV capabilities of *Swift*/UVOT also enable the dust content along the line of sight to be studied, and photometric redshifts to be obtained for GRBs where a spectroscopic redshift has not been possible.

Swift/UVOT will continue to build the samples of the optical/UV light curves required to explain the collective behaviours of GRBs, and to continue to observe and to detect unique GRBs and transients that push the boundaries of our understanding. There are still many questions to be addressed regarding long GRBs, such as when is the onset of the afterglow for ∼80% of GRBs, what is the structure of the jet, and whether there is any variation in observer viewing angle; *Swift* will continue to provide exquisite data to address these issues.

Funding: This research received no external funding.

Data Availability Statement: The data presented in Section 3.1 of this review are openly available at https://swift.gsfc.nasa.gov/archive/grb_table/, accessed 20th October 2022. For all other sections, no new data were created nor analysed, and data sharing is not applicable.

Acknowledgments: The author would like to acknowledge and thank all the engineers and scientists that built and calibrated *Swift*/UVOT, analysed *Swift*/UVOT GRB data, and supported and planned *Swift*/UVOT observations. This review paper would not be possible without their time and dedication. This research has made use of data obtained from the High Energy Astrophysics Science Archive Research Center (HEASARC) and the Leicester Database and Archive Service (LEDAS), provided by NASA's Goddard Space Flight Center and the School of Physics and Astronomy, University of Leicester, UK, respectively.

Conflicts of Interest: The author declares no conflicts of interest.

Abbreviations

The following abbreviations are used in this manuscript:

GRB	Gamma-ray burst
IR	Infrared
LGRB	Long gamma-ray burst
SGRB	Short gamma-ray burst
SN(e)	Supernova(e)
UV	Ultra-violet
UVOT	Ultra-Violet/Optical Telescope
XRT	X-Ray Telescope

References

1. Sari, R. Hydrodynamics of Gamma-Ray Burst Afterglow. *Astrophys. J. Lett.* **1997**, *489*, L37–L40. [CrossRef]
2. Sari, R.; Piran, T.; Narayan, R. Spectra and Light Curves of Gamma-Ray Burst Afterglows. *Astrophys. J. Lett.* **1998**, *497*, L17–L20.
3. Kouveliotou, C.; Meegan, C.A.; Fishman, G.J.; Bhat, N.P.; Briggs, M.S.; Koshut, T.M.; Paciesas, W.S.; Pendleton, G.N. Identification of two classes of gamma-ray bursts. *Astrophys. J. Lett.* **1993**, *413*, L101–L104. [CrossRef]
4. Paczynski, B. Gamma-ray bursters at cosmological distances. *Astrophys. J. Lett.* **1986**, *308*, L43–L46. [CrossRef]
5. Eichler, D.; Livio, M.; Piran, T.; Schramm, D.N. Nucleosynthesis, neutrino bursts and gamma-rays from coalescing neutron stars. *Nature* **1989**, *340*, 126–128. [CrossRef]
6. Abbott, B.P.; Abbott, R.; Abbott, T.D.; Acernese, F.; Ackley, K.; Adams, C.; Adams, T.; Addesso, P.; Adhikari, R.X.; Adya, V.B.; et al. Multi-messenger Observations of a Binary Neutron Star Merger. *Astrophys. J. Lett.* **2017**, *848*, L12.
7. Abbott, B.P.; Abbott, R.; Abbott, T.D.; Acernese, F.; Ackley, K.; Adams, C.; Adams, T.; Addesso, P.; Adhikari, R.X.; Adya, V.B.; et al. Gravitational Waves and Gamma-Rays from a Binary Neutron Star Merger: GW170817 and GRB 170817A. *Astrophys. J. Lett.* **2017**, *848*, L13.
8. Coulter, D.A.; Foley, R.J.; Kilpatrick, C.D.; Drout, M.R.; Piro, A.L.; Shappee, B.J.; Siebert, M.R.; Simon, J.D.; Ulloa, N.; Kasen, D.; et al. Swope Supernova Survey 2017a (SSS17a), the optical counterpart to a gravitational wave source. *Science* **2017**, *358*, 1556–1558.
9. Evans, P.A.; Cenko, S.B.; Kennea, J.A.; Emery, S.W.K.; Kuin, N.P.M.; Korobkin, O.; Wollaeger, R.T.; Fryer, C.L.; Madsen, K.K.; Harrison, F.A.; et al. Swift and NuSTAR observations of GW170817: Detection of a blue kilonova. *Science* **2017**, *358*, 1565–1570.
10. Goldstein, A.; Veres, P.; Burns, E.; Briggs, M.S.; Hamburg, R.; Kocevski, D.; Wilson-Hodge, C.A.; Preece, R.D.; Poolakkil, S.; Roberts, O.J.; et al. An Ordinary Short Gamma-Ray Burst with Extraordinary Implications: Fermi-GBM Detection of GRB 170817A. *Astrophys. J. Lett.* **2017**, *848*, L14.
11. Woosley, S.E. Gamma-ray bursts from stellar mass accretion disks around black holes. *Astrophys. J.* **1993**, *405*, 273–277. [CrossRef]
12. MacFadyen, A.I.; Woosley, S.E. Collapsars: Gamma-Ray Bursts and Explosions in "Failed Supernovae". *Astrophys. J.* **1999**, *524*, 262–289.
13. Galama, T.J.; Vreeswijk, P.M.; van Paradijs, J.; Kouveliotou, C.; Augusteijn, T.; Böhnhardt, H.; Brewer, J.P.; Doublier, V.; Gonzalez, J.F.; Leibundgut, B.; et al. An unusual supernova in the error box of the γ-ray burst of 25 April 1998. *Nature* **1998**, *395*, 670–672.
14. Kulkarni, S.R.; Frail, D.A.; Wieringa, M.H.; Ekers, R.D.; Sadler, E.M.; Wark, R.M.; Higdon, J.L.; Phinney, E.S.; Bloom, J.S. Radio emission from the unusual supernova 1998bw and its association with the γ-ray burst of 25 April 1998. *Nature* **1998**, *395*, 663–669. [CrossRef]
15. Hjorth, J.; Sollerman, J.; Møller, P.; Fynbo, J.P.U.; Woosley, S.E.; Kouveliotou, C.; Tanvir, N.R.; Greiner, J.; Andersen, M.I.; Castro-Tirado, A.J.; et al. A very energetic supernova associated with the γ-ray burst of 29 March 2003. *Nature* **2003**, *423*, 847–850.
16. Woosley, S.E.; Bloom, J.S. The Supernova Gamma-Ray Burst Connection. *Ann. Rev. Astron. Astrophys.* **2006**, *44*, 507–556.
17. Gehrels, N.; Chincarini, G.; Giommi, P.; Mason, K.O.; Nousek, J.A.; Wells, A.A.; White, N.E.; Barthelmy, S.D.; Burrows, D.N.; Cominsky, L.R.; et al. The Swift Gamma-Ray Burst Mission. *Astrophys. J.* **2004**, *611*, 1005–1020. [CrossRef]
18. Bromberg, O.; Nakar, E.; Piran, T.; Sari, R. Short versus Long and Collapsars versus Non-collapsars: A Quantitative Classification of Gamma-Ray Bursts. *Astrophys. J.* **2013**, *764*, 179.
19. Della Valle, M.; Malesani, D.; Bloom, J.S.; Benetti, S.; Chincarini, G.; D'Avanzo, P.; Foley, R.J.; Covino, S.; Melandri, A.; Piranomonte, S.; et al. Hypernova Signatures in the Late Rebrightening of GRB 050525A. *Astrophys. J. Lett.* **2006**, *642*, L103–L106.
20. Fynbo, J.P.U.; Watson, D.; Thöne, C.C.; Sollerman, J.; Bloom, J.S.; Davis, T.M.; Hjorth, J.; Jakobsson, P.; Jørgensen, U.G.; Graham, J.F.; et al. No supernovae associated with two long-duration γ-ray bursts. *Nature* **2006**, *444*, 1047–1049. [CrossRef]
21. Gehrels, N.; Norris, J.P.; Barthelmy, S.D.; Granot, J.; Kaneko, Y.; Kouveliotou, C.; Markwardt, C.B.; Mészáros, P.; Nakar, E.; Nousek, J.A.; et al. A new γ-ray burst classification scheme from GRB060614. *Nature* **2006**, *444*, 1044–1046.
22. Gal-Yam, A.; Fox, D.B.; Price, P.A.; Ofek, E.O.; Davis, M.R.; Leonard, D.C.; Soderberg, A.M.; Schmidt, B.P.; Lewis, K.M.; Peterson, B.A.; et al. A novel explosive process is required for the γ-ray burst GRB 060614. *Nature* **2006**, *444*, 1053–1055.
23. Ahumada, T.; Singer, L.P.; Anand, S.; Coughlin, M.W.; Kasliwal, M.M.; Ryan, G.; Andreoni, I.; Cenko, S.B.; Fremling, C.; Kumar, H.; et al. Discovery and confirmation of the shortest gamma-ray burst from a collapsar. *Nat. Astron.* **2021**, *5*, 917–927.

24. Zhang, B.B.; Liu, Z.K.; Peng, Z.K.; Li, Y.; Lü, H.J.; Yang, J.; Yang, Y.S.; Yang, Y.H.; Meng, Y.Z.; Zou, J.H.; et al. A peculiarly short-duration gamma-ray burst from massive star core collapse. *Nat. Astron.* **2021**, *5*, 911–916.
25. Rossi, A.; Rothberg, B.; Palazzi, E.; Kann, D.A.; D'Avanzo, P.; Amati, L.; Klose, S.; Perego, A.; Pian, E.; Guidorzi, C.; et al. The Peculiar Short-duration GRB 200826A and Its Supernova. *Astrophys. J.* **2022**, *932*, 1.
26. Rastinejad, J.C.; Gompertz, B.P.; Levan, A.J.; Fong, W.F.; Nicholl, M.; Lamb, G.P.; Malesani, D.B.; Nugent, A.E.; Oates, S.R.; Tanvir, N.R.; et al. A kilonova following a long-duration gamma-ray burst at 350 Mpc. *Nature* **2022**, *612*, 223–227.
27. Troja, E.; Fryer, C.L.; O'Connor, B.; Ryan, G.; Dichiara, S.; Kumar, A.; Ito, N.; Gupta, R.; Wollaeger, R.T.; Norris, J.P.; et al. A nearby long gamma-ray burst from a merger of compact objects. *Nature* **2022**, *612*, 228–231.
28. Yang, J.; Ai, S.; Zhang, B.B.; Zhang, B.; Liu, Z.K.; Wang, X.I.; Yang, Y.H.; Yin, Y.H.; Li, Y.; Lü, H.J. A long-duration gamma-ray burst with a peculiar origin. *Nature* **2022**, *612*, 232–235.
29. Sakamoto, T.; Pal'Shin, V.; Yamaoka, K.; Ohno, M.; Sato, G.; Aptekar, R.; Barthelmy, S.D.; Baumgartner, W.H.; Cummings, J.R.; Fenimore, E.E.; et al. Spectral Cross-Calibration of the Konus-Wind, the Suzaku/WAM, and the Swift/BAT Data Using Gamma-Ray Bursts. *Publ. Astron. Soc. Jpn.* **2011**, *63*, 215.
30. Savchenko, V.; Neronov, A.; Courvoisier, T.J.L. Timing properties of gamma-ray bursts detected by SPI-ACS detector onboard INTEGRAL. *Astron. Astrophys.* **2012**, *541*, A122.
31. Qin, Y.; Liang, E.W.; Liang, Y.F.; Yi, S.X.; Lin, L.; Zhang, B.B.; Zhang, J.; Lü, H.J.; Lu, R.J.; Lü, L.Z.; et al. A Comprehensive Analysis of Fermi Gamma-Ray Burst Data. III. Energy-dependent T_{90} Distributions of GBM GRBs and Instrumental Selection Effect on Duration Classification. *Astrophys. J.* **2013**, *763*, 15.
32. Zhang, B. Astrophysics: A burst of new ideas. *Nature* **2006**, *444*, 1010–1011.
33. Klebesadel, R.W.; Strong, I.B.; Olson, R.A. Observations of Gamma-Ray Bursts of Cosmic Origin. *Astrophys. J. Lett.* **1973**, *182*, L85–L88. [CrossRef]
34. Meegan, C.A.; Fishman, G.J.; Wilson, R.B.; Horack, J.M.; Brock, M.N.; Paciesas, W.S.; Pendleton, G.N.; Kouveliotou, C. Spatial distribution of gamma-ray bursts observed by BATSE. *Nature* **1992**, *355*, 143–145. [CrossRef]
35. Liang, E.P. Plasma radiation during gamma-ray bursts. *Nature* **1985**, *313*, 202–204. [CrossRef]
36. Hartmann, D.; Woosley, S.E.; Arons, J. Thermal cyclotron reprocessing of gamma-ray bursts—Theory and model spectra. *Astrophys. J.* **1988**, *332*, 777–803. [CrossRef]
37. Rappaport, S.A.; Joss, P.C. On the binary nature of cosmic gamma-ray burst sources. *Nature* **1985**, *314*, 242–245. [CrossRef]
38. Boella, G.; Butler, R.C.; Perola, G.C.; Piro, L.; Scarsi, L.; Bleeker, J.A.M. BeppoSAX, the wide band mission for X-ray astronomy. *Astr. Astrophys. Suppl.* **1997**, *122*, 299–307. [CrossRef]
39. Parmar, A.N.; Martin, D.D.E.; Bavdaz, M.; Favata, F.; Kuulkers, E.; Vacanti, G.; Lammers, U.; Peacock, A.; Taylor, B.G. The low-energy concentrator spectrometer on-board the BeppoSAX X-ray astronomy satellite. *Astr. Astrophys. Suppl.* **1997**, *122*, 309–326. [CrossRef]
40. Boella, G.; Chiappetti, L.; Conti, G.; Cusumano, G.; del Sordo, S.; La Rosa, G.; Maccarone, M.C.; Mineo, T.; Molendi, S.; Re, S.; et al. The medium-energy concentrator spectrometer on board the BeppoSAX X-ray astronomy satellite. *Astr. Astrophys. Suppl.* **1997**, *122*, 327–340. [CrossRef]
41. Frontera, F.; Costa, E.; dal Fiume, D.; Feroci, M.; Nicastro, L.; Orlandini, M.; Palazzi, E.; Zavattini, G. The high energy instrument PDS on-board the BeppoSAX X–ray astronomy satellite. *Astr. Astrophys. Suppl.* **1997**, *122*, 357–369. [CrossRef]
42. Costa, E.; Frontera, F.; Heise, J.; Feroci, M.; in't Zand, J.; Fiore, F.; Cinti, M.N.; Dal Fiume, D.; Nicastro, L.; Orlandini, M.; et al. Discovery of an X-ray afterglow associated with the γ-ray burst of 28 February 1997. *Nature* **1997**, *387*, 783–785.
43. van Paradijs, J.; Groot, P.J.; Galama, T.; Kouveliotou, C.; Strom, R.G.; Telting, J.; Rutten, R.G.M.; Fishman, G.J.; Meegan, C.A.; Pettini, M.; et al. Transient optical emission from the error box of the γ-ray burst of 28 February 1997. *Nature* **1997**, *386*, 686–689. [CrossRef]
44. Metzger, M.R.; Djorgovski, S.G.; Kulkarni, S.R.; Steidel, C.C.; Adelberger, K.L.; Frail, D.A.; Costa, E.; Frontera, F. Spectral constraints on the redshift of the optical counterpart to the γ-ray burst of 8 May 1997. *Nature* **1997**, *387*, 878–880. [CrossRef]
45. Pian, E.; Amati, L.; Antonelli, L.A.; Butler, R.C.; Costa, E.; Cusumano, G.; Danziger, J.; Feroci, M.; Fiore, F.; Frontera, F.; et al. BeppoSAX detection and follow-up of GRB 980425. *Astr. Astrophys. Suppl.* **1999**, *138*, 463–464. [CrossRef]
46. Katz, J.I.; Piran, T. Persistent Counterparts to Gamma-Ray Bursts. *Astrophys. J.* **1997**, *490*, 772. [CrossRef]
47. Kobayashi, S.; Piran, T.; Sari, R. Can Internal Shocks Produce the Variability in Gamma-Ray Bursts? *Astrophys. J.* **1997**, *490*, 92. [CrossRef]
48. Kobayashi, S.; Ryde, F.; MacFadyen, A. Luminosity and Variability of Collimated Gamma-Ray Bursts. *Astrophys. J.* **2002**, *577*, 302–310.
49. Rhoads, J.E. How to Tell a Jet from a Balloon: A Proposed Test for Beaming in Gamma-Ray Bursts. *Astrophys. J. Lett.* **1997**, *487*, L1.
50. Piran, T. Gamma-ray bursts and the fireball model. *Phys. Rep.* **1999**, *314*, 575–667. [CrossRef]
51. Rhoads, J.E. The Dynamics and Light Curves of Beamed Gamma-Ray Burst Afterglows. *Astrophys. J.* **1999**, *525*, 737–749.
52. Sari, R.; Piran, T. Predictions for the Very Early Afterglow and the Optical Flash. *Astrophys. J.* **1999**, *520*, 641–649.
53. Zeh, A.; Klose, S.; Kann, D.A. Gamma-Ray Burst Afterglow Light Curves in the Pre-Swift Era: A Statistical Study. *Astrophys. J.* **2006**, *637*, 889–900.

54. Lamb, D.Q. The Role of Dust in GRB Afterglows. In *Gamma-Ray Burst and Afterglow Astronomy 2001: A Workshop Celebrating the First Year of the HETE Mission*; American Institute of Physics Conference Series; Ricker, G.R., Vanderspek, R.K., Eds.; AIP Conference Proceedings: Melville, NY, USA, 2003; Volume 662, pp. 415–416.
55. Crew, G.B.; Lamb, D.Q.; Ricker, G.R.; Atteia, J.L.; Kawai, N.; Vanderspek, R.; Villasenor, J.; Doty, J.; Prigozhin, G.; Jernigan, J.G.; et al. HETE-2 Localization and Observation of the Bright, X-Ray-rich Gamma-Ray Burst GRB 021211. *Astrophys. J.* **2003**, *599*, 387–393.
56. Pandey, S.B.; Anupama, G.C.; Sagar, R.; Bhattacharya, D.; Castro-Tirado, A.J.; Sahu, D.K.; Parihar, P.; Prabhu, T.P. The optical afterglow of the not so dark GRB 021211. *Astron. Astrophys.* **2003**, *408*, L21–L24. [CrossRef]
57. Groot, P.J.; Galama, T.J.; Vreeswijk, P.M.; Wijers, R.A.M.J.; Pian, E.; Palazzi, E.; van Paradijs, J.; Kouveliotou, C.; Zand, J.J.M.I.; Heise, J.; et al. The Rapid Decay of the Optical Emission from GRB 980326 and Its Possible Implications. *Astrophys. J. Lett.* **1998**, *502*, L123–L127.
58. Barthelmy, S.D.; Barbier, L.M.; Cummings, J.R.; Fenimore, E.E.; Gehrels, N.; Hullinger, D.; Krimm, H.A.; Markwardt, C.B.; Palmer, D.M.; Parsons, A.; et al. The Burst Alert Telescope (BAT) on the SWIFT Midex Mission. *Space Sci. Rev.* **2005**, *120*, 143–164.
59. Burrows, D.N.; Hill, J.E.; Nousek, J.A.; Kennea, J.A.; Wells, A.; Osborne, J.P.; Abbey, A.F.; Beardmore, A.; Mukerjee, K.; Short, A.D.T.; et al. The Swift X-Ray Telescope. *Space Sci. Rev.* **2005**, *120*, 165–195.
60. Roming, P.W.A.; Kennedy, T.E.; Mason, K.O.; Nousek, J.A.; Ahr, L.; Bingham, R.E.; Broos, P.S.; Carter, M.J.; Hancock, B.K.; Huckle, H.E.; et al. The Swift Ultra-Violet/Optical Telescope. *Space Sci. Rev.* **2005**, *120*, 95–142.
61. Oates, S.R.; Page, M.J.; De Pasquale, M.; Schady, P.; Breeveld, A.A.; Holland, S.T.; Kuin, N.P.M.; Marshall, F.E. A correlation between the intrinsic brightness and average decay rate of Swift/UVOT gamma-ray burst optical/ultraviolet light curves. *Mon. Not. R. Astr. Soc.* **2012**, *426*, L86–L90.
62. Roming, P.W.A.; Koch, T.S.; Oates, S.R.; Porterfield, B.L.; Bayless, A.J.; Breeveld, A.A.; Gronwall, C.; Kuin, N.P.M.; Page, M.J.; de Pasquale, M.; et al. A Large Catalog of Homogeneous Ultra-Violet/Optical GRB Afterglows: Temporal and Spectral Evolution. *Astrophys. J. Suppl.* **2017**, *228*, 13.
63. Page, M.J.; Oates, S.R.; De Pasquale, M.; Breeveld, A.A.; Emery, S.W.K.; Kuin, N.P.M.; Marshall, F.E.; Siegel, M.H.; Roming, P.W.A. A study of gamma-ray burst afterglows as they first come into view of the Swift Ultraviolet and Optical Telescope. *Mon. Not. R. Astr. Soc.* **2019**, *488*, 2855–2863.
64. Poole, T.S.; Breeveld, A.A.; Page, M.J.; Landsman, W.; Holland, S.T.; Roming, P.; Kuin, N.P.M.; Brown, P.J.; Gronwall, C.; Hunsberger, S.; et al. Photometric calibration of the Swift ultraviolet/optical telescope. *Mon. Not. R. Astr. Soc.* **2008**, *383*, 627–645.
65. Breeveld, A.A.; Landsman, W.; Holland, S.T.; Roming, P.; Kuin, N.P.M.; Page, M.J. An Updated Ultraviolet Calibration for the Swift/UVOT. In *American Institute of Physics Conference Series*; McEnery, J.E., Racusin, J.L., Gehrels, N., Eds.; AIP Conference Proceedings: Melville, NY, USA, 2011; Volume 1358, pp. 373–376.
66. Cenko, S.B.; Kelemen, J.; Harrison, F.A.; Fox, D.B.; Kulkarni, S.R.; Kasliwal, M.M.; Ofek, E.O.; Rau, A.; Gal-Yam, A.; Frail, D.A.; et al. Dark Bursts in the Swift Era: The Palomar 60 Inch-Swift Early Optical Afterglow Catalog. *Astrophys. J.* **2009**, *693*, 1484–1493.
67. Greiner, J.; Krühler, T.; Klose, S.; Afonso, P.; Clemens, C.; Filgas, R.; Hartmann, D.H.; Küpcü Yoldaş, A.; Nardini, M.; Olivares, E.F.; et al. The nature of "dark" gamma-ray bursts. *Astron. Astrophys.* **2011**, *526*, A30.
68. Kuin, N.P.M.; Landsman, W.; Breeveld, A.A.; Page, M.J.; Lamoureux, H.; James, C.; Mehdipour, M.; Still, M.; Yershov, V.; Brown, P.J.; et al. Calibration of the Swift-UVOT ultraviolet and visible grisms. *Mon. Not. R. Astr. Soc.* **2015**, *449*, 2514–2538.
69. Kuin, N.P.M.; Landsman, W.; Page, M.J.; Schady, P.; Still, M.; Breeveld, A.A.; de Pasquale, M.; Roming, P.W.A.; Brown, P.J.; Carter, M.; et al. GRB 081203A: Swift UVOT captures the earliest ultraviolet spectrum of a gamma-ray burst. *Mon. Not. R. Astr. Soc.* **2009**, *395*, L21–L24.
70. Maselli, A.; Melandri, A.; Nava, L.; Mundell, C.G.; Kawai, N.; Campana, S.; Covino, S.; Cummings, J.R.; Cusumano, G.; Evans, P.A.; et al. GRB 130427A: A Nearby Ordinary Monster. *Science* **2014**, *343*, 48–51.
71. De Pasquale, M.; Oates, S.R.; Page, M.J.; Burrows, D.N.; Blustin, A.J.; Zane, S.; Mason, K.O.; Roming, P.W.A.; Palmer, D.; Gehrels, N.; et al. Early afterglow detection in the Swift observations of GRB 050801. *Mon. Not. R. Astr. Soc.* **2007**, *377*, 1638–1646.
72. Krühler, T.; Schady, P.; Greiner, J.; Afonso, P.; Bottacini, E.; Clemens, C.; Filgas, R.; Klose, S.; Koch, T.S.; Küpcü-Yoldaş, A.; et al. Photometric redshifts for gamma-ray burst afterglows from GROND and Swift/UVOT. *Astron. Astrophys.* **2011**, *526*, A153.
73. Gupta, R.; Oates, S.R.; Pandey, S.B.; Castro-Tirado, A.J.; Joshi, J.C.; Hu, Y.D.; Valeev, A.F.; Zhang, B.B.; Zhang, Z.; Kumar, A.; et al. GRB 140102A: insight into prompt spectral evolution and early optical afterglow emission. *Mon. Not. R. Astr. Soc.* **2021**, *505*, 4086–4105.
74. Still, M.; Roming, P.W.A.; Mason, K.O.; Blustin, A.; Boyd, P.; Breeveld, A.; Brown, P.; De Pasquale, M.; Gronwall, C.; Holland, S.T.; et al. Swift UVOT Detection of GRB 050318. *Astrophys. J.* **2005**, *635*, 1187–1191.
75. Schady, P.; de Pasquale, M.; Page, M.J.; Vetere, L.; Pandey, S.B.; Wang, X.Y.; Cummings, J.; Zhang, B.; Zane, S.; Breeveld, A.; et al. Extreme properties of GRB061007: a highly energetic or a highly collimated burst? *Mon. Not. R. Astr. Soc.* **2007**, *380*, 1041–1052.
76. Mundell, C.G.; Melandri, A.; Guidorzi, C.; Kobayashi, S.; Steele, I.A.; Malesani, D.; Amati, L.; D'Avanzo, P.; Bersier, D.F.; Gomboc, A.; et al. The Remarkable Afterglow of GRB 061007: Implications for Optical Flashes and GRB Fireballs. *Astrophys. J.* **2007**, *660*, 489–495.
77. Jakobsson, P.; Fynbo, J.P.U.; Tanvir, N.; Rol, E. GRB 061007: OA fading and VLT redshift. *GRB Coord. Netw.* **2006**, *5716*, 1.

78. Golenetskii, S.; Aptekar, R.; Mazets, E.; Pal'Shin, V.; Frederiks, D.; Cline, T. Konus-wind observation of GRB 061007. *GRB Coord. Netw.* **2006**, *5722*, 1.
79. Vreeswijk, P.M.; Smette, A.; Malesani, D.; Fynbo, J.P.U.; Milvang-Jensen, B.; Jakobsson, P.; Jaunsen, A.O.; Ledoux, C. VLT/UVES redshift of GRB 080319B. *GRB Coord. Netw.* **2008**, *7444*, 1.
80. Racusin, J.L.; Karpov, S.V.; Sokolowski, M.; Granot, J.; Wu, X.F.; Pal'Shin, V.; Covino, S.; van der Horst, A.J.; Oates, S.R.; Schady, P.; et al. Broadband observations of the naked-eye γ-ray burst GRB080319B. *Nature* **2008**, *455*, 183–188.
81. Levan, A.J.; Cenko, S.B.; Perley, D.A.; Tanvir, N.R. GRB 130427A: gemini-north redshift. *GRB Coord. Netw.* **2013**, *14455*, 1.
82. Dirirsa, F.; Racusin, J.; McEnery, J.; Desiante, R. GRB 160625B: Fermi-LAT detection of a bright burst. *GRB Coord. Netw.* **2016**, *19580*, 1.
83. Burns, E. GRB 160625B: Fermi GBM initial observations. *GRB Coord. Netw.* **2016**, *19581*, 1.
84. Ajello, M.; Arimoto, M.; Axelsson, M.; Baldini, L.; Barbiellini, G.; Bastieri, D.; Bellazzini, R.; Berretta, A.; Bissaldi, E.; Blandford, R.D.; et al. Fermi and Swift Observations of GRB 190114C: Tracing the Evolution of High-energy Emission from Prompt to Afterglow. *Astrophys. J.* **2020**, *890*, 9.
85. MAGIC Collaboration.; Acciari, V.A.; Ansoldi, S.; Antonelli, L.A.; Arbet Engels, A.; Baack, D.; Babić, A.; Banerjee, B.; Barres de Almeida, U.; Barrio, J.A.; et al. Teraelectronvolt emission from the γ-ray burst GRB 190114C. *Nature* **2019**, *575*, 455–458.
86. Dichiara, S.; Gropp, J.D.; Kennea, J.A.; Kuin, N.P.M.; Lien, A.Y.; Marshall, F.E.; Tohuvavohu, A.; Williams, M.A.; Neil Gehrels Swift Observatory Team. Swift J1913.1+1946 a new bright hard X-ray and optical transient. *GRB Coord. Netw.* **2022**, *32632*, 1.
87. Kennea, J.A.; Williams, M.; Swift Team. GRB 221009A: Swift detected transient may be GRB. *GRB Coord. Netw.* **2022**, *32635*, 1.
88. de Ugarte Postigo, A.; Izzo, L.; Pugliese, G.; Xu, D.; Schneider, B.; Fynbo, J.P.U.; Tanvir, N.R.; Malesani, D.B.; Saccardi, A.; Kann, D.A.; et al. GRB 221009A: Redshift from X-shooter/VLT. *GRB Coord. Netw.* **2022**, *32648*, 1.
89. Castro-Tirado, A.J.; Sanchez-Ramirez, R.; Hu, Y.D.; Caballero-Garcia, M.D.; Castro Tirado, M.A.; Fernandez-Garcia, E.; Perez-Garcia, I.; Lombardi, G.; Pandey, S.B.; Yang, J.; et al. GRB 221009A: 10.4m GTC spectroscopic redshift confirmation. *GRB Coord. Netw.* **2022**, *32686*, 1.
90. Malesani, D.B.; Levan, A.J.; Izzo, L.; de, Ugarte, Postigo, A.; Ghirl, a, G.; Heintz, K.E.; Kann, D.A.; Lamb, G.P.; Palmerio, J.; Salafia, O.S.; et al. The brightest GRB ever detected: GRB 221009A as a highly luminous event at z = 0.151. *arXiv* **2023**, arXiv:2302.07891.
91. Veres, P.; Burns, E.; Bissaldi, E.; Lesage, S.; Roberts, O.; Fermi GBM Team. GRB 221009A: Fermi GBM detection of an extraordinarily bright GRB. *GRB Coord. Netw.* **2022**, *32636*, 1.
92. Bissaldi, E.; Omodei, N.; Kerr, M.; Fermi-LAT Team. GRB 221009A or Swift J1913.1+1946: Fermi-LAT detection. *GRB Coord. Netw.* **2022**, *32637*, 1.
93. Ursi, A.; Panebianco, G.; Pittori, C.; Verrecchia, F.; Longo, F.; Parmiggiani, N.; Tavani, M.; Argan, A.; Cardillo, M.; Casentini, C.; et al. GRB 221009A (Swift J1913.1+1946): AGILE/MCAL detection. *GRB Coord. Netw.* **2022**, *32650*, 1.
94. Gotz, D.; Mereghetti, S.; Savchenko, V.; Ferrigno, C.; Bozzo, E.; IBAS Team. GRB221009A/Swift J1913.1+1946: INTEGRAL SPI/ACS observations. *GRB Coord. Netw.* **2022**, *32660*, 1.
95. Xiao, H.; Krucker, S.; Daniel, R. GRB221009A/Swift J1913.1+1946: Solar Orbiter STIX measurements. *GRB Coord. Netw.* **2022**, *32661*, 1.
96. Frederiks, D.; Lysenko, A.; Ridnaia, A.; Svinkin, D.; Tsvetkova, A.; Ulanov, M.; Cline, T.; Konus-Wind Team. Konus-Wind detection of GRB 221009A. *GRB Coord. Netw.* **2022**, *32668*, 1.
97. Ripa, J.; Pal, A.; Werner, N.; Ohno, M.; Takahashi, H.; Meszaros, L.; B., C.; Dafcikova, M.; et al. GRB 221009A: Detection by GRBAlpha. *GRB Coord. Netw.* **2022**, *32685*, 1.
98. Liu, J.C.; Zhang, Y.Q.; Xiong, S.L.; Zheng, C.; Wang, C.W.; Xue, W.C.; Qiao, R.; J., T.W.; Zhang, D.L.; et al. GRB 221009A: HEBS detection. *GRB Coord. Netw.* **2022**, *32751*, 1.
99. Huang, Y.; Hu, S.; Chen, S.; Zha, M.; Liu, C.; Yao, Z.; Cao, Z.; Experiment, T.L. LHAASO observed GRB 221009A with more than 5000 VHE photons up to around 18 TeV. *GRB Coord. Netw.* **2022**, *32677*, 1.
100. Dzhappuev, D.D.; Afashokov, Y.Z.; Dzaparova, I.M.; Dzhatdoev, T.A.; Gorbacheva, E.A.; Karpikov, I.S.; Khadzhiev, M.M.; Klimenko, N.F.; Kudzhaev, A.U.; Kurenya, A.N.; et al. Swift J1913.1+1946/GRB 221009A: detection of a 250-TeV photon-like air shower by Carpet-2. *Astron. Telegr.* **2022**, *15669*, 1.
101. Kann, D.A.; Agui Fernandez, J.F. GRB 221009A: Armchair Energetics. *GRB Coord. Netw.* **2022**, *32762*, 1.
102. Kann, D.A.; Agayeva, S.; Aivazyan, V.; Alishov, S.; Andrade, C.M.; Antier, S.; Baransky, A.; Bendjoya, P.; Benkhaldoun, Z.; Beradze, S.; et al. GRANDMA and HXMT Observations of GRB 221009A—The Standard-Luminosity Afterglow of a Hyper-Luminous Gamma-Ray Burst. *arXiv* **2023**, arXiv:2302.06225.
103. Williams, M.A.; Kennea, J.A.; Dichiara, S.; Kobayashi, K.; Iwakiri, W.B.; Beardmore, A.P.; Evans, P.A.; Heinz, S.; Lien, A.; Oates, S.R.; et al. GRB 221009A: Discovery of an Exceptionally Rare Nearby and Energetic Gamma-Ray Burst. *arXiv* **2023**, arXiv:2302.03642.
104. Levan, A.J.; Lamb, G.P.; Schneider, B.; Hjorth, J.; Zafar, T.; de, Ugarte, Postigo, A.; Sargent, B.; Mullally, S.E.; Izzo, L.; D'Avanzo, P.; et al. The first JWST spectrum of a GRB afterglow: No bright supernova in observations of the brightest GRB of all time, GRB 221009A. *arXiv* **2023**, arXiv:2302.07761.
105. O'Connor, B.; Troja, E.; Ryan, G.; Beniamini, P.; van, Eerten, H.; Granot, J.; Dichiara, S.; Ricci, R.; Lipunov, V.; Gillanders, J.H.; et al. A structured jet explains the extreme GRB 221009A. *arXiv* **2023**, arXiv:2302.07906.

106. Ripa, J.; Takahashi, H.; Fukazawa, Y.; Werner, N.; Munz, F.; Pal, A.; Ohno, M.; Dafcikova, M.; Meszaros, L.; Csak, B.; et al. The peak-flux of GRB 221009A measured with GRBAlpha. *arXiv* **2023**, arXiv:2302.10047.
107. Ai, S.; Gao, H. Model constraints based on the IceCube neutrino non-detection of GRB 221009A. *arXiv* **2022**, arXiv:2210.14116.
108. Alves Batista, R. GRB 221009A: A potential source of ultra-high-energy cosmic rays. *arXiv* **2022**, arXiv:2210.12855.
109. Carenza, P.; Marsh, M.C.D. On ALP scenarios and GRB 221009A. *arXiv* **2022**, arXiv:2211.02010.
110. Cheung, K. The Role of a Heavy Neutrino in the Gamma-Ray Burst GRB-221009A. *arXiv* **2022**, arXiv:2210.14178.
111. Galanti, G.; Roncadelli, M.; Tavecchio, F. Assessment of ALP scenarios for GRB 221009A. *arXiv* **2022**, arXiv:2211.06935.
112. González, M.M.; Avila Rojas, D.; Pratts, A.; Hernández-Cadena, S.; Fraija, N.; Alfaro, R.; Pérez Araujo, Y.; Montes, J.A. GRB 221009A: A light dark matter burst or an extremely bright Inverse Compton component? *arXiv* **2022**, arXiv:2210.15857.
113. Li, H.; Ma, B.Q. Lorentz invariance violation induced threshold anomaly versus very-high energy cosmic photon emission from GRB 221009A. *arXiv* **2022**, arXiv:2210.06338.
114. Murase, K.; Mukhopadhyay, M.; Kheirandish, A.; Kimura, S.S.; Fang, K. Neutrinos from the Brightest Gamma-Ray Burst? *Astrophys. J. Lett.* **2022**, *941*, L10.
115. Nakagawa, S.; Takahashi, F.; Yamada, M.; Yin, W. Axion dark matter from first-order phase transition, and very high energy photons from GRB 221009A. *arXiv* **2022**, arXiv:2210.10022.
116. Ren, J.; Wang, Y.; Zhang, L.L. Very High Energy Afterglow Emission of GRB~221009A: Lessons Learned from the Brightest Long Gamma-ray Burst in a Wind Environment. *arXiv* **2022**, arXiv:2210.10673.
117. Romanov, F. The contribution of the modern amateur astronomer to the science of astronomy. *arXiv* **2022**, arXiv:2212.12543.
118. Rudolph, A.; Petropoulou, M.; Bošnjak, Ž.; Winter, W. Multi-collision internal shock lepto-hadronic models for energetic GRBs. *arXiv* **2022**, arXiv:2212.00765.
119. Rudolph, A.; Petropoulou, M.; Winter, W.; Bošnjak, Ž. Multi-messenger model for the prompt emission from GRB 221009A. *arXiv* **2022**, arXiv:2212.00766.
120. Sato, Y.; Murase, K.; Ohira, Y.; Yamazaki, R. Two-component jet model for multi-wavelength afterglow emission of the extremely energetic burst GRB 221009A. *arXiv* **2022**, arXiv:2212.09266.
121. Smirnov, A.Y.; Trautner, A. GRB 221009A Gamma Rays from Radiative Decay of Heavy Neutrinos? *arXiv* **2022**, arXiv:2211.00634.
122. Vardanyan, V.; Takhistov, V.; Ata, M.; Murase, K. Revisiting Tests of Lorentz Invariance with Gamma-ray Bursts: Effects of Intrinsic Lags. *arXiv* **2022**, arXiv:2212.02436.
123. Xia, Z.Q.; Wang, Y.; Yuan, Q.; Fan, Y.Z. An inter-galactic magnetic field strength of $\sim 4 \times 10^{-17}$ G inferred with GRB 221009A. 2022, *pre-print*.
124. Zhang, B.T.; Murase, K.; Ioka, K.; Song, D.; Yuan, C.; Mészáros, P. External Inverse-Compton and Proton Synchrotron Emission from the Reverse Shock as the Origin of VHE Gamma-Rays from the Hyper-Bright GRB 221009A. *arXiv* **2022**, arXiv:2211.05754.
125. Zheng, Y.G.; Kang, S.J.; Zhu, K.R.; Yang, C.Y.; Bai, J.M. Expected Signature for the Lorentz Invariance Violation Effects on $\gamma - \gamma$ Absorption. *arXiv* **2022**, arXiv:2211.01836.
126. Zhu, J.; Ma, B.Q. Light speed variation from GRB 221009A. *arXiv* **2022**, arXiv:2210.11376.
127. Abbasi, R.; Ackermann, M.; Adams, J.; Agarwalla, S.; Aggarwal, N.; Aguilar, J.A.; Ahlers, M.; Alameddine, J.M.; Amin, N.M.; Andeen, K.; et al. Limits on Neutrino Emission from GRB 221009A from MeV to PeV using the IceCube Neutrino Observatory. *arXiv* **2023**, arXiv:2302.05459.
128. Camisasca, A.E.; Guidorzi, C.; Amati, L.; Frontera, F.; Song, X.Y.; Xiao, S.; Xiong, S.L.; Zhang, S.N.; Margutti, R.; Kobayashi, S.; et al. GRB minimum variability timescale with Insight-HXMT and Swift: implications for progenitor models, dissipation physics and GRB classifications. *arXiv* **2023**, arXiv:2301.01176.
129. Das, S.; Razzaque, S. Ultrahigh-energy cosmic-ray signature in GRB 221009A. *Astron. Astrophys.* **2023**, *670*, L12.
130. Finke, J.D.; Razzaque, S. Possible Evidence for Lorentz Invariance Violation in Gamma-Ray Burst 221009A. *Astrophys. J. Lett.* **2023**, *942*, L21.
131. Fulton, M.D.; Smartt, S.J.; Rhodes, L.; Huber, M.E.; Villar, A.V.; Moore, T.; Srivastav, S.; Schultz, A.S.B.; Chambers, K.C.; Izzo, L.; et al. The optical light curve of GRB 221009A: The afterglow and detection of the emerging supernova SN 2022xiw. *arXiv* **2023**, arXiv:2301.11170.
132. Guarini, E.; Tamborra, I.; Bégué, D.; Rudolph, A. Probing gamma-ray bursts observed at very high energies through their afterglow. *arXiv* **2023**, arXiv:2301.10256.
133. Laskar, T.; Alexander, K.D.; Margutti, R.; Eftekhari, T.; Chornock, R.; Berger, E.; Cendes, Y.; Duerr, A.; Perley, D.A.; Edvige Ravasio, M.; et al. The Radio to GeV Afterglow of GRB 221009A. *arXiv* **2023**, arXiv:2302.04388.
134. Liu, R.Y.; Zhang, H.M.; Wang, X.Y. Constraints on Gamma-Ray Burst Models from GRB 221009A: GeV Gamma Rays versus High-energy Neutrinos. *Astrophys. J. Lett.* **2023**, *943*, L2.
135. Negro, M.; Di Lalla, N.; Omodei, N.; Veres, P.; Silvestri, S.; Manfreda, A.; Burns, E.; Baldini, L.; Costa, E.; Ehlert, S.R.; et al. The IXPE view of GRB 221009A. *arXiv* **2023**, arXiv:2301.01798.
136. Sahu, S.; Medina-Carrillo, B.; Sánchez-Colón, G.; Rajpoot, S. Deciphering the 18 TeV Photons from GRB 221009A. *Astrophys. J. Lett.* **2023**, *942*, L30.
137. Shrestha, M.; Sand, D.J.; Alexander, K.D.; Bostroem, K.A.; Hosseinzadeh, G.; Pearson, J.; Aghakhanloo, M.; Vinkó, J.; Andrews, J.E.; Jencson, J.E.; et al. Lack of Bright Supernova Emission in the Brightest Gamma-ray Burst, GRB~221009A. *arXiv* **2023**, arXiv:2302.03829.

138. Vasilopoulos, G.; Karavola, D.; Stathopoulos, S.I.; Petropoulou, M. Dust-scattering rings of GRB 221009A as seen by the Neil Gehrels Swift satellite: can we count them all? *Mon. Not. R. Astron. Soc.* **2023**, stad375.
139. Zhao, Z.C.; Zhou, Y.; Wang, S. Multi-TeV photons from GRB 221009A: Uncertainty of optical depth considered. *Eur. Phys. J. C* **2023**, *83*, 92.
140. Zhang, G.; Ma, B.Q. Axion-Photon Conversion of LHAASO Multi-TeV and PeV Photons. *Chin. Phys. Lett.* **2023**, *40*, 011401.
141. Tinney, C.; Stathakis, R.; Cannon, R.; Galama, T.; Wieringa, M.; Frail, D.A.; Kulkarni, S.R.; Higdon, J.L.; Wark, R.; Bloom, J.S.; et al. GRB 980425. *Int. Astron. Union Circ.* **1998**, *6896*, 3.
142. Foley, S.; Watson, D.; Gorosabel, J.; Fynbo, J.P.U.; Sollerman, J.; McGlynn, S.; McBreen, B.; Hjorth, J. The galaxies in the field of the nearby GRB 980425/SN 1998bw. *Astron. Astrophys.* **2006**, *447*, 891–895. [CrossRef]
143. Prochaska, J.X.; Bloom, J.S.; Chen, H.W.; Hurley, K.C.; Melbourne, J.; Dressler, A.; Graham, J.R.; Osip, D.J.; Vacca, W.D. The Host Galaxy of GRB 031203: Implications of Its Low Metallicity, Low Redshift, and Starburst Nature. *Astrophys. J.* **2004**, *611*, 200–207.
144. Margutti, R.; Chincarini, G.; Covino, S.; Tagliaferri, G.; Campana, S.; Della Valle, M.; Filippenko, A.V.; Fiore, F.; Foley, R.; Fugazza, D.; et al. The host galaxy of GRB 031203: a new spectroscopic study. *Astron. Astrophys.* **2007**, *474*, 815–826. [CrossRef]
145. Greiner, J.; Peimbert, M.; Esteban, C.; Kaufer, A.; Jaunsen, A.; Smoke, J.; Klose, S.; Reimer, O. Redshift of GRB 030329. *GRB Coord. Netw.* **2003**, *2020*, 1.
146. Thöne, C.C.; Greiner, J.; Savaglio, S.; Jehin, E. ISM Studies of GRB 030329 with High-Resolution Spectroscopy. *Astrophys. J.* **2007**, *671*, 628–636.
147. Mirabal, N.; Halpern, J.P. GRB 060218: MDM redshift. *GRB Coord. Netw.* **2006**, *4792*, 1.
148. Starling, R.L.C.; Wiersema, K.; Levan, A.J.; Sakamoto, T.; Bersier, D.; Goldoni, P.; Oates, S.R.; Rowlinson, A.; Campana, S.; Sollerman, J.; et al. Discovery of the nearby long, soft GRB 100316D with an associated supernova. *Mon. Not. R. Astr. Soc.* **2011**, *411*, 2792–2803.
149. MichałowskI, M.J.; Xu, D.; Stevens, J.; Levan, A.; Yang, J.; Paragi, Z.; Kamble, A.; Tsai, A.L.; Dannerbauer, H.; van der Horst, A.J.; et al. The second-closest gamma-ray burst: sub-luminous GRB 111005A with no supernova in a super-solar metallicity environment. *Astron. Astrophys.* **2018**, *616*, A169.
150. Tanga, M.; Krühler, T.; Schady, P.; Klose, S.; Graham, J.F.; Greiner, J.; Kann, D.A.; Nardini, M. The environment of the SN-less GRB 111005A at z = 0.0133. *Astron. Astrophys.* **2018**, *615*, A136.
151. Campana, S.; Mangano, V.; Blustin, A.J.; Brown, P.; Burrows, D.N.; Chincarini, G.; Cummings, J.R.; Cusumano, G.; Della Valle, M.; Malesani, D.; et al. The association of GRB 060218 with a supernova and the evolution of the shock wave. *Nature* **2006**, *442*, 1008–1010.
152. Pian, E.; Mazzali, P.A.; Masetti, N.; Ferrero, P.; Klose, S.; Palazzi, E.; Ramirez-Ruiz, E.; Woosley, S.E.; Kouveliotou, C.; Deng, J.; et al. An optical supernova associated with the X-ray flash XRF 060218. *Nature* **2006**, *442*, 1011–1013.
153. Emery, S.W.K.; Page, M.J.; Breeveld, A.A.; Brown, P.J.; Kuin, N.P.M.; Oates, S.R.; De Pasquale, M. The early optical afterglow and non-thermal components of GRB 060218. *Mon. Not. R. Astr. Soc.* **2019**, *484*, 5484–5498. [CrossRef]
154. Gendre, B.; Stratta, G.; Atteia, J.L.; Basa, S.; Boër, M.; Coward, D.M.; Cutini, S.; D'Elia, V.; Howell, E.J.; Klotz, A.; et al. The Ultra-long Gamma-Ray Burst 111209A: The Collapse of a Blue Supergiant? *Astrophys. J.* **2013**, *766*, 30.
155. Levan, A.J.; Tanvir, N.R.; Starling, R.L.C.; Wiersema, K.; Page, K.L.; Perley, D.A.; Schulze, S.; Wynn, G.A.; Chornock, R.; Hjorth, J.; et al. A New Population of Ultra-long Duration Gamma-Ray Bursts. *Astrophys. J.* **2014**, *781*, 13. [CrossRef]
156. Kann, D.A.; Schady, P.; Olivares, E.F.; Klose, S.; Rossi, A.; Perley, D.A.; Zhang, B.; Krühler, T.; Greiner, J.; Nicuesa Guelbenzu, A.; et al. The optical/NIR afterglow of GRB 111209A: Complex yet not unprecedented. *Astron. Astrophys.* **2018**, *617*, A122. [CrossRef]
157. Thöne, C.C.; de Ugarte Postigo, A.; Fryer, C.L.; Page, K.L.; Gorosabel, J.; Aloy, M.A.; Perley, D.A.; Kouveliotou, C.; Janka, H.T.; Mimica, P.; et al. The unusual γ-ray burst GRB 101225A from a helium star/neutron star merger at redshift 0.33. *Nature* **2011**, *480*, 72–74.
158. Campana, S.; Lodato, G.; D'Avanzo, P.; Panagia, N.; Rossi, E.M.; Della Valle, M.; Tagliaferri, G.; Antonelli, L.A.; Covino, S.; Ghirlanda, G.; et al. The unusual gamma-ray burst GRB 101225A explained as a minor body falling onto a neutron star. *Nature* **2011**, *480*, 69–71.
159. Vreeswijk, P.; Fynbo, J.; Melandri, A. GRB 111209A: VLT/X-shooter redshift. *GRB Coord. Netw.* **2011**, *12648*, 1.
160. Stratta, G.; Gendre, B.; Atteia, J.L.; Boër, M.; Coward, D.M.; De Pasquale, M.; Howell, E.; Klotz, A.; Oates, S.; Piro, L. The Ultra-long GRB 111209A. II. Prompt to Afterglow and Afterglow Properties. *Astrophys. J.* **2013**, *779*, 66.
161. Vreeswijk, P.M.; Malesani, D.; Fynbo, J.P.U.; De Cia, A.; Ledoux, C. GRB 130925A: VLT/UVES observations. *GRB Coord. Netw.* **2013**, *15249*, 1.
162. Evans, P.A.; Willingale, R.; Osborne, J.P.; O'Brien, P.T.; Tanvir, N.R.; Frederiks, D.D.; Pal'shin, V.D.; Svinkin, D.S.; Lien, A.; Cummings, J.; et al. GRB 130925A: an ultralong gamma ray burst with a dust-echo afterglow, and implications for the origin of the ultralong GRBs. *Mon. Not. R. Astr. Soc.* **2014**, *444*, 250–267.
163. Greiner, J.; Yu, H.F.; Krühler, T.; Frederiks, D.D.; Beloborodov, A.; Bhat, P.N.; Bolmer, J.; van Eerten, H.; Aptekar, R.L.; Elliott, J.; et al. GROND coverage of the main peak of gamma-ray burst 130925A. *Astron. Astrophys.* **2014**, *568*, A75.
164. Marshall, F.E.; Evans, P.A. GRB 121027A: Swift/UVOT possible detection. *GRB Coord. Netw.* **2012**, *13932*, 1.
165. Amati, L.; Frontera, F.; Tavani, M.; in't Zand, J.J.M.; Antonelli, A.; Costa, E.; Feroci, M.; Guidorzi, C.; Heise, J.; Masetti, N.; et al. Intrinsic spectra and energetics of BeppoSAX Gamma-Ray Bursts with known redshifts. *Astron. Astrophys.* **2002**, *390*, 81–89. [CrossRef]

166. Ghirlanda, G.; Ghisellini, G.; Lazzati, D. The Collimation-corrected Gamma-Ray Burst Energies Correlate with the Peak Energy of Their νF Spectrum. *Astrophys. J.* **2004**, *616*, 331–338.
167. Schlafly, E.F.; Finkbeiner, D.P. Measuring Reddening with Sloan Digital Sky Survey Stellar Spectra and Recalibrating SFD. *Astrophys. J.* **2011**, *737*, 103.
168. van der Horst, A.J.; Kouveliotou, C.; Gehrels, N.; Rol, E.; Wijers, R.A.M.J.; Cannizzo, J.K.; Racusin, J.; Burrows, D.N. Optical Classification of Gamma-Ray Bursts in the Swift Era. *Astrophys. J.* **2009**, *699*, 1087–1091.
169. Melandri, A.; Mundell, C.G.; Kobayashi, S.; Guidorzi, C.; Gomboc, A.; Steele, I.A.; Smith, R.J.; Bersier, D.; Mottram, C.J.; Carter, D.; et al. The Early-Time Optical Properties of Gamma-Ray Burst Afterglows. *Astrophys. J.* **2008**, *686*, 1209–1230.
170. Zheng, W.K.; Deng, J.S.; Wang, J. Statistical studies of optically dark gamma-ray bursts in the Swift era. *Res. Astron. Astrophys.* **2009**, *9*, 1103–1118.
171. Melandri, A.; Sbarufatti, B.; D'Avanzo, P.; Salvaterra, R.; Campana, S.; Covino, S.; Vergani, S.D.; Nava, L.; Ghisellini, G.; Ghirlanda, G.; et al. The dark bursts population in a complete sample of bright Swift long gamma-ray bursts. *Mon. Not. R. Astr. Soc.* **2012**, *421*, 1265–1272.
172. Fynbo, J.P.U.; Jakobsson, P.; Prochaska, J.X.; Malesani, D.; Ledoux, C.; de Ugarte Postigo, A.; Nardini, M.; Vreeswijk, P.M.; Wiersema, K.; Hjorth, J.; et al. Low-resolution Spectroscopy of Gamma-ray Burst Optical Afterglows: Biases in the Swift Sample and Characterization of the Absorbers. *Astrophys. J. Suppl.* **2009**, *185*, 526–573.
173. Fynbo, J.U.; Jensen, B.L.; Gorosabel, J.; Hjorth, J.; Pedersen, H.; Møller, P.; Abbott, T.; Castro-Tirado, A.J.; Delgado, D.; Greiner, J.; et al. Detection of the optical afterglow of GRB 000630: Implications for dark bursts. *Astron. Astrophys.* **2001**, *369*, 373–379. [CrossRef]
174. Roming, P.W.A.; Schady, P.; Fox, D.B.; Zhang, B.; Liang, E.; Mason, K.O.; Rol, E.; Burrows, D.N.; Blustin, A.J.; Boyd, P.T.; et al. Very Early Optical Afterglows of Gamma-Ray Bursts: Evidence for Relative Paucity of Detection. *Astrophys. J.* **2006**, *652*, 1416–1422.
175. D'Elia, V.; Stratta, G. GRB 100614A and GRB 100615A: two extremely dark gamma-ray bursts. *Astron. Astrophys.* **2011**, *532*, A48.
176. Jeong, S.; Castro-Tirado, A.J.; Bremer, M.; Winters, J.M.; Gorosabel, J.; Guziy, S.; Pandey, S.B.; Jelínek, M.; Sánchez-Ramírez, R.; Sokolov, I.V.; et al. The dark nature of GRB 130528A and its host galaxy. *Astron. Astrophys.* **2014**, *569*, A93.
177. Chrimes, A.A.; Levan, A.J.; Stanway, E.R.; Berger, E.; Bloom, J.S.; Cenko, S.B.; Cobb, B.E.; Cucchiara, A.; Fruchter, A.S.; Gompertz, B.P.; et al. The case for a high-redshift origin of GRB 100205A. *Mon. Not. R. Astr. Soc.* **2019**, *488*, 902–909.
178. Perley, D.A.; Cenko, S.B.; Bloom, J.S.; Chen, H.W.; Butler, N.R.; Kocevski, D.; Prochaska, J.X.; Brodwin, M.; Glazebrook, K.; Kasliwal, M.M.; et al. The Host Galaxies of Swift Dark Gamma-ray Bursts: Observational Constraints on Highly Obscured and Very High Redshift GRBs. *Astron. J.* **2009**, *138*, 1690–1708.
179. Zhang, B.; Mészáros, P. Gamma-Ray Burst Afterglow with Continuous Energy Injection: Signature of a Highly Magnetized Millisecond Pulsar. *Astrophys. J. Lett.* **2001**, *552*, L35–L38.
180. Rees, M.J.; Meszaros, P. Refreshed Shocks and Afterglow Longevity in Gamma-Ray Bursts. *Astrophys. J. Lett.* **1998**, *496*, L1.
181. Nousek, J.A.; Kouveliotou, C.; Grupe, D.; Page, K.L.; Granot, J.; Ramirez-Ruiz, E.; Patel, S.K.; Burrows, D.N.; Mangano, V.; Barthelmy, S.; et al. Evidence for a Canonical Gamma-Ray Burst Afterglow Light Curve in the Swift XRT Data. *Astrophys. J.* **2006**, *642*, 389–400.
182. Zhang, B.; Fan, Y.Z.; Dyks, J.; Kobayashi, S.; Mészáros, P.; Burrows, D.N.; Nousek, J.A.; Gehrels, N. Physical Processes Shaping Gamma-Ray Burst X-Ray Afterglow Light Curves: Theoretical Implications from the Swift X-ray Telescope Observations. *Astrophys. J.* **2006**, *642*, 354–370. [CrossRef]
183. Oates, S.R.; Page, M.J.; Schady, P.; De Pasquale, M.; Koch, T.S.; Breeveld, A.A.; Brown, P.J.; Chester, M.M.; Holland, S.T.; Hoversten, E.A.; et al. A statistical study of gamma-ray burst afterglows measured by the Swift Ultraviolet Optical Telescope. *Mon. Not. R. Astr. Soc.* **2009**, *395*, 490–503.
184. Evans, P.A.; Beardmore, A.P.; Page, K.L.; Osborne, J.P.; O'Brien, P.T.; Willingale, R.; Starling, R.L.C.; Burrows, D.N.; Godet, O.; Vetere, L.; et al. Methods and results of an automatic analysis of a complete sample of Swift-XRT observations of GRBs. *Mon. Not. R. Astr. Soc.* **2009**, *397*, 1177–1201.
185. Li, L.; Liang, E.W.; Tang, Q.W.; Chen, J.M.; Xi, S.Q.; Lü, H.J.; Gao, H.; Zhang, B.; Zhang, J.; Yi, S.X.; et al. A Comprehensive Study of Gamma-Ray Burst Optical Emission. I. Flares and Early Shallow-decay Component. *Astrophys. J.* **2012**, *758*, 27.
186. Liang, E.W.; Yi, S.X.; Zhang, J.; Lü, H.J.; Zhang, B.B.; Zhang, B. Constraining Gamma-ray Burst Initial Lorentz Factor with the Afterglow Onset Feature and Discovery of a Tight Γ_0-E $_{\gamma,iso}$ Correlation. *Astrophys. J.* **2010**, *725*, 2209–2224.
187. Panaitescu, A.; Vestrand, W.T. Optical afterglows of gamma-ray bursts: Peaks, plateaus and possibilities. *Mon. Not. R. Astr. Soc.* **2011**, *414*, 3537–3546.
188. Liang, E.W.; Li, L.; Gao, H.; Zhang, B.; Liang, Y.F.; Wu, X.F.; Yi, S.X.; Dai, Z.G.; Tang, Q.W.; Chen, J.M.; et al. A Comprehensive Study of Gamma-Ray Burst Optical Emission. II. Afterglow Onset and Late Re-brightening Components. *Astrophys. J.* **2013**, *774*, 13.
189. Kopač, D.; Kobayashi, S.; Gomboc, A.; Japelj, J.; Mundell, C.G.; Guidorzi, C.; Melandri, A.; Bersier, D.; Cano, Z.; Smith, R.J.; et al. GRB 090727 and Gamma-Ray Bursts with Early-time Optical Emission. *Astrophys. J.* **2013**, *772*, 73.
190. Page, K.L.; Willingale, R.; Osborne, J.P.; Zhang, B.; Godet, O.; Marshall, F.E.; Melandri, A.; Norris, J.P.; O'Brien, P.T.; Pal'shin, V.; et al. GRB 061121: Broadband Spectral Evolution through the Prompt and Afterglow Phases of a Bright Burst. *Astrophys. J.* **2007**, *663*, 1125–1138.

191. Oganesyan, G.; Nava, L.; Ghirlanda, G.; Melandri, A.; Celotti, A. Prompt optical emission as a signature of synchrotron radiation in gamma-ray bursts. *Astron. Astrophys.* **2019**, *628*, A59.
192. Rossi, A.; Schulze, S.; Klose, S.; Kann, D.A.; Rau, A.; Krimm, H.A.; Jóhannesson, G.; Panaitescu, A.; Yuan, F.; Ferrero, P.; et al. The Swift/Fermi GRB 080928 from 1 eV to 150 keV. *Astron. Astrophys.* **2011**, *529*, A142.
193. Zhang, B.; Kobayashi, S.; Mészáros, P. Gamma-Ray Burst Early Optical Afterglows: Implications for the Initial Lorentz Factor and the Central Engine. *Astrophys. J.* **2003**, *595*, 950–954.
194. Zhang, B.; Kobayashi, S. Gamma-Ray Burst Early Afterglows: Reverse Shock Emission from an Arbitrarily Magnetized Ejecta. *Astrophys. J.* **2005**, *628*, 315–334.
195. Gomboc, A.; Kobayashi, S.; Mundell, C.G.; Guidorzi, C.; Melandri, A.; Steele, I.A.; Smith, R.J.; Bersier, D.; Carter, D.; Bode, M.F. Optical flashes, reverse shocks and magnetization. In *Gamma-Ray Burst: Sixth Huntsville Symposium*; American Institute of Physics Conference Series; Meegan, C., Kouveliotou, C., Gehrels, N., Eds.; AIP Conference Proceedings: Melville, NY, USA, 2009; Volume 1133, pp. 145–150.
196. Gao, H.; Wang, X.G.; Mészáros, P.; Zhang, B. A Morphological Analysis of Gamma-Ray Burst Early-optical Afterglows. *Astrophys. J.* **2015**, *810*, 160.
197. Oates, S.R.; Page, M.J.; Schady, P.; de Pasquale, M.; Evans, P.A.; Page, K.L.; Chester, M.M.; Curran, P.A.; Koch, T.S.; Kuin, N.P.M.; et al. A statistical comparison of the optical/UV and X-ray afterglows of gamma-ray bursts using the Swift Ultraviolet Optical and X-ray Telescopes. *Mon. Not. R. Astr. Soc.* **2011**, *412*, 561–579.
198. Willingale, R.; Mészáros, P. Gamma-Ray Bursts and Fast Transients. Multi-wavelength Observations and Multi-messenger Signals. *Space Sci. Rev.* **2017**, *207*, 63–86. [CrossRef]
199. Molinari, E.; Vergani, S.D.; Malesani, D.; Covino, S.; D'Avanzo, P.; Chincarini, G.; Zerbi, F.M.; Antonelli, L.A.; Conconi, P.; Testa, V.; et al. REM observations of GRB 060418 and GRB 060607A: The onset of the afterglow and the initial fireball Lorentz factor determination. *Astron. Astrophys.* **2007**, *469*, L13–L16. [CrossRef]
200. Rykoff, E.S.; Aharonian, F.; Akerlof, C.W.; Ashley, M.C.B.; Barthelmy, S.D.; Flewelling, H.A.; Gehrels, N.; Göğüş, E.; Güver, T.; Kiziloğlu, Ü.; et al. Looking Into the Fireball: ROTSE-III and Swift Observations of Early Gamma-ray Burst Afterglows. *Astrophys. J.* **2009**, *702*, 489–505.
201. Sari, R.; Piran, T.; Halpern, J.P. Jets in Gamma-Ray Bursts. *Astrophys. J. Lett.* **1999**, *519*, L17–L20.
202. Kobayashi, S. Light Curves of Gamma-Ray Burst Optical Flashes. *Astrophys. J.* **2000**, *545*, 807–812.
203. Panaitescu, A.; Kumar, P. Analytic Light Curves of Gamma-Ray Burst Afterglows: Homogeneous versus Wind External Media. *Astrophys. J.* **2000**, *543*, 66–76.
204. Meszaros, P. Gamma-ray bursts. *Rep. Prog. Phys.* **2006**, *69*, 2259–2322. [CrossRef]
205. Fenimore, E.E.; Epstein, R.I.; Ho, C. The escape of 100 MeV photons from cosmological gamma-ray bursts. *Astr. Astrophys. Suppl.* **1993**, *97*, 59–62.
206. Piran, T. The physics of gamma-ray bursts. *Rev. Mod. Phys.* **2004**, *76*, 1143–1210.
207. Rees, M.J.; Meszaros, P. Relativistic fireballs-Energy conversion and time-scales. *Mon. Not. R. Astr. Soc.* **1992**, *258*, 41P–43P. [CrossRef]
208. Meszaros, P.; Rees, M.J. Optical and Long-Wavelength Afterglow from Gamma-Ray Bursts. *Astrophys. J.* **1997**, *476*, 232.
209. Rees, M.J.; Meszaros, P. Unsteady outflow models for cosmological gamma-ray bursts. *Astrophys. J. Lett.* **1994**, *430*, L93–L96.
210. Piro, L.; Amati, L.; Antonelli, L.A.; Butler, R.C.; Costa, E.; Cusumano, G.; Feroci, M.; Frontera, F.; Heise, J.; in 't Zand, J.J.M.; et al. Evidence for a late-time outburst of the X-ray afterglow of GB970508 from BeppoSAX. *Astron. Astrophys.* **1998**, *331*, L41–L44.
211. Piro, L.; De Pasquale, M.; Soffitta, P.; Lazzati, D.; Amati, L.; Costa, E.; Feroci, M.; Frontera, F.; Guidorzi, C.; in't Zand, J.M.J.; et al. Probing the Environment in Gamma-Ray Bursts: The Case of an X-Ray Precursor, Afterglow Late Onset, and Wind Versus Constant Density Profile in GRB 011121 and GRB 011211. *Astrophys. J.* **2005**, *623*, 314–324.
212. Burrows, D.N.; Romano, P.; Falcone, A.; Kobayashi, S.; Zhang, B.; Moretti, A.; O'Brien, P.T.; Goad, M.R.; Campana, S.; Page, K.L.; et al. Bright X-ray Flares in Gamma-Ray Burst Afterglows. *Science* **2005**, *309*, 1833–1835. [CrossRef]
213. Roming, P.W.A.; Vanden Berk, D.; Pal'shin, V.; Pagani, C.; Norris, J.; Kumar, P.; Krimm, H.; Holland, S.T.; Gronwall, C.; Blustin, A.J.; et al. GRB 060313: A New Paradigm for Short-Hard Bursts? *Astrophys. J.* **2006**, *651*, 985–993. [CrossRef]
214. O'Brien, P.T.; Willingale, R.; Osborne, J.; Goad, M.R.; Page, K.L.; Vaughan, S.; Rol, E.; Beardmore, A.; Godet, O.; Hurkett, C.P.; et al. The Early X-ray Emission from GRBs. *Astrophys. J.* **2006**, *647*, 1213–1237.
215. Falcone, A.D.; Morris, D.; Racusin, J.; Chincarini, G.; Moretti, A.; Romano, P.; Burrows, D.N.; Pagani, C.; Stroh, M.; Grupe, D.; et al. The First Survey of X-ray Flares from Gamma-Ray Bursts Observed by Swift: Spectral Properties and Energetics. *Astrophys. J.* **2007**, *671*, 1921–1938.
216. Chincarini, G.; Moretti, A.; Romano, P.; Falcone, A.D.; Morris, D.; Racusin, J.; Campana, S.; Covino, S.; Guidorzi, C.; Tagliaferri, G.; et al. The First Survey of X-ray Flares from Gamma-Ray Bursts Observed by Swift: Temporal Properties and Morphology. *Astrophys. J.* **2007**, *671*, 1903–1920.
217. Swenson, C.A.; Roming, P.W.A.; De Pasquale, M.; Oates, S.R. Gamma-Ray Burst Flares: Ultraviolet/Optical Flaring. I. *Astrophys. J.* **2013**, *774*, 2.
218. Yi, S.X.; Yu, H.; Wang, F.Y.; Dai, Z.G. Statistical Distributions of Optical Flares from Gamma-Ray Bursts. *Astrophys. J.* **2017**, *844*, 79.

219. Swenson, C.A.; Maxham, A.; Roming, P.W.A.; Schady, P.; Vetere, L.; Zhang, B.B.; Zhang, B.; Holland, S.T.; Kennea, J.A.; Kuin, N.P.M.; et al. GRB 090926A and Bright Late-time Fermi Large Area Telescope Gamma-ray Burst Afterglows. *Astrophys. J. Lett.* **2010**, *718*, L14–L18.
220. Nardini, M.; Elliott, J.; Filgas, R.; Schady, P.; Greiner, J.; Krühler, T.; Klose, S.; Afonso, P.; Kann, D.A.; Nicuesa Guelbenzu, A.; et al. Afterglow rebrightenings as a signature of a long-lasting central engine activity? The emblematic case of GRB 100814A. *Astron. Astrophys.* **2014**, *562*, A29.
221. De Pasquale, M.; Kuin, N.P.M.; Oates, S.; Schulze, S.; Cano, Z.; Guidorzi, C.; Beardmore, A.; Evans, P.A.; Uhm, Z.L.; Zhang, B.; et al. The optical rebrightening of GRB100814A: an interplay of forward and reverse shocks? *Mon. Not. R. Astr. Soc.* **2015**, *449*, 1024–1042.
222. Granot, J.; Panaitescu, A.; Kumar, P.; Woosley, S.E. Off-Axis Afterglow Emission from Jetted Gamma-Ray Bursts. *Astrophys. J. Lett.* **2002**, *570*, L61–L64.
223. Oates, S.R.; De Pasquale, M.; Page, M.J.; Blustin, A.J.; Zane, S.; McGowan, K.; Mason, K.O.; Poole, T.S.; Schady, P.; Roming, P.W.A.; et al. The two-component afterglow of Swift GRB 050802. *Mon. Not. R. Astr. Soc.* **2007**, *380*, 270–280.
224. De Pasquale, M.; Evans, P.; Oates, S.; Page, M.; Zane, S.; Schady, P.; Breeveld, A.; Holland, S.; Kuin, P.; Still, M.; et al. Jet breaks at the end of the slow decline phase of Swift GRB light curves. *Mon. Not. R. Astr. Soc.* **2009**, *392*, 153–169.
225. Frail, D.A.; Kulkarni, S.R.; Sari, R.; Djorgovski, S.G.; Bloom, J.S.; Galama, T.J.; Reichart, D.E.; Berger, E.; Harrison, F.A.; Price, P.A.; et al. Beaming in Gamma-Ray Bursts: Evidence for a Standard Energy Reservoir. *Astrophys. J. Lett.* **2001**, *562*, L55–L58.
226. Bloom, J.S.; Frail, D.A.; Sari, R. The Prompt Energy Release of Gamma-Ray Bursts using a Cosmological k-Correction. *Astron. J.* **2001**, *121*, 2879–2888.
227. Kulkarni, S.R.; Djorgovski, S.G.; Odewahn, S.C.; Bloom, J.S.; Gal, R.R.; Koresko, C.D.; Harrison, F.A.; Lubin, L.M.; Armus, L.; Sari, R.; et al. The afterglow, redshift and extreme energetics of the γ-ray burst of 23 January 1999. *Nature* **1999**, *398*, 389–394.
228. Harrison, F.A.; Yost, S.A.; Sari, R.; Berger, E.; Galama, T.J.; Holtzman, J.; Axelrod, T.; Bloom, J.S.; Chevalier, R.; Costa, E.; et al. Broadband Observations of the Afterglow of GRB 000926: Observing the Effect of Inverse Compton Scattering. *Astrophys. J.* **2001**, *559*, 123–130. [CrossRef]
229. Klose, S.; Greiner, J.; Rau, A.; Henden, A.A.; Hartmann, D.H.; Zeh, A.; Ries, C.; Masetti, N.; Malesani, D.; Guenther, E.; et al. Probing a Gamma-Ray Burst Progenitor at a Redshift of z = 2: A Comprehensive Observing Campaign of the Afterglow of GRB 030226. *Astron. J.* **2004**, *128*, 1942–1954.
230. Blustin, A.J.; Band, D.; Barthelmy, S.; Boyd, P.; Capalbi, M.; Holland, S.T.; Marshall, F.E.; Mason, K.O.; Perri, M.; Poole, T.; et al. Swift Panchromatic Observations of the Bright Gamma-Ray Burst GRB 050525a. *Astrophys. J.* **2006**, *637*, 901–913.
231. Hu, Y.D.; Oates, S.R.; Lipunov, V.M.; Zhang, B.B.; Castro-Tirado, A.J.; Jeong, S.; Sánchez-Ramírez, R.; Tello, J.C.; Cunniffe, R.; Gorbovskoy, E.; et al. Multiwavelength observations of GRB 140629A. A long burst with an achromatic jet break in the optical and X-ray afterglow. *Astron. Astrophys.* **2019**, *632*, A100.
232. Burrows, D.N.; Racusin, J. Swift X-ray afterglows: Where are the X-ray jet breaks? *Nuovo C. B Ser.* **2006**, *121*, 1273–1287.
233. Liang, E.; Racusin, J.L.; Zhang, B.; Zhang, B.; Burrows, D.N. A Comprehensive Analysis of Swift XRT Data. III. Jet Break Candidates in X-Ray and Optical Afterglow Light Curves. *Astrophys. J.* **2008**, *675*, 528–552.
234. Racusin, J.L.; Liang, E.W.; Burrows, D.N.; Falcone, A.; Sakamoto, T.; Zhang, B.B.; Zhang, B.; Evans, P.; Osborne, J. Jet Breaks and Energetics of Swift Gamma-ray Burst X-ray Afterglows. *Astrophys. J.* **2009**, *698*, 43–74.
235. Grupe, D.; Gronwall, C.; Wang, X.; Roming, P.W.A.; Cummings, J.; Zhang, B.; Mészáros, P.; Trigo, M.D.; O'Brien, P.T.; Page, K.L.; et al. Swift and XMM-Newton Observations of the Extraordinary Gamma-Ray Burst 060729: More than 125 Days of X-Ray Afterglow. *Astrophys. J.* **2007**, *662*, 443–458.
236. Wang, X.G.; Zhang, B.; Liang, E.W.; Gao, H.; Li, L.; Deng, C.M.; Qin, S.M.; Tang, Q.W.; Kann, D.A.; Ryde, F.; et al. How Bad or Good Are the External Forward Shock Afterglow Models of Gamma-Ray Bursts? *Astrophys. J. Suppl.* **2015**, *219*, 9.
237. Wang, X.G.; Zhang, B.; Liang, E.W.; Lu, R.J.; Lin, D.B.; Li, J.; Li, L. Gamma-Ray Burst Jet Breaks Revisited. *Astrophys. J.* **2018**, *859*, 160.
238. Zhao, W.; Zhang, J.C.; Zhang, Q.X.; Liang, J.T.; Luan, X.H.; Zhou, Q.Q.; Yi, S.X.; Wang, F.F.; Zhang, S.T. Statistical Study of Gamma-Ray Bursts with Jet Break Features in Multiwavelength Afterglow Emissions. *Astrophys. J.* **2020**, *900*, 112.
239. Zhang, B.; Liang, E.; Page, K.L.; Grupe, D.; Zhang, B.B.; Barthelmy, S.D.; Burrows, D.N.; Campana, S.; Chincarini, G.; Gehrels, N.; et al. GRB Radiative Efficiencies Derived from the Swift Data: GRBs versus XRFs, Long versus Short. *Astrophys. J.* **2007**, *655*, 989–1001.
240. Racusin, J.L.; Oates, S.R.; Schady, P.; Burrows, D.N.; de Pasquale, M.; Donato, D.; Gehrels, N.; Koch, S.; McEnery, J.; Piran, T.; et al. Fermi and Swift Gamma-ray Burst Afterglow Population Studies. *Astrophys. J.* **2011**, *738*, 138.
241. Liang, E.; Zhang, B. Model-independent Multivariable Gamma-Ray Burst Luminosity Indicator and Its Possible Cosmological Implications. *Astrophys. J.* **2005**, *633*, 611–623.
242. Guetta, D.; Granot, J.; Begelman, M.C. Constraining the Structure of Gamma-Ray Burst Jets through the logN-logS Distribution. *Astrophys. J.* **2005**, *622*, 482–491.
243. Nardini, M.; Ghisellini, G.; Ghirlanda, G.; Tavecchio, F.; Firmani, C.; Lazzati, D. Clustering of the optical-afterglow luminosities of long gamma-ray bursts. *Astron. Astrophys.* **2006**, *451*, 821–833. [CrossRef]
244. Nardini, M.; Ghisellini, G.; Ghirlanda, G. Optical afterglow luminosities in the Swift epoch: confirming clustering and bimodality. *Mon. Not. R. Astr. Soc.* **2008**, *386*, L87–L91.

245. Liang, E.; Zhang, B. Identification of Two Categories of Optically Bright Gamma-Ray Bursts. *Astrophys. J. Lett.* **2006**, *638*, L67–L70.
246. Kann, D.A.; Klose, S.; Zhang, B.; Malesani, D.; Nakar, E.; Pozanenko, A.; Wilson, A.C.; Butler, N.R.; Jakobsson, P.; Schulze, S.; et al. The Afterglows of Swift-era Gamma-ray Bursts. I. Comparing pre-Swift and Swift-era Long/Soft (Type II) GRB Optical Afterglows. *Astrophys. J.* **2010**, *720*, 1513–1558.
247. Kann, D.A.; Klose, S.; Zhang, B.; Covino, S.; Butler, N.R.; Malesani, D.; Nakar, E.; Wilson, A.C.; Antonelli, L.A.; Chincarini, G.; et al. The Afterglows of Swift-era Gamma-Ray Bursts. II. Type I GRB versus Type II GRB Optical Afterglows. *Astrophys. J.* **2011**, *734*, 96.
248. Zaninoni, E.; Bernardini, M.G.; Margutti, R.; Oates, S.; Chincarini, G. Gamma-ray burst optical light-curve zoo: comparison with X-ray observations. *Astron. Astrophys.* **2013**, *557*, A12.
249. Kann, D.A.; Blazek, M.; de Ugarte Postigo, A.; Thöne, C.C. GN-z11-flash in the Context of Gamma-Ray Burst Afterglows. *Res. Notes Am. Astron. Soc.* **2020**, *4*, 247.
250. Bernardini, M.G.; Margutti, R.; Mao, J.; Zaninoni, E.; Chincarini, G. The X-ray light curve of gamma-ray bursts: Clues to the central engine. *Astron. Astrophys.* **2012**, *539*, A3.
251. Margutti, R.; Zaninoni, E.; Bernardini, M.G.; Chincarini, G.; Pasotti, F.; Guidorzi, C.; Angelini, L.; Burrows, D.N.; Capalbi, M.; Evans, P.A.; et al. The prompt-afterglow connection in gamma-ray bursts: a comprehensive statistical analysis of Swift X-ray light curves. *Mon. Not. R. Astr. Soc.* **2013**, *428*, 729–742.
252. Zaninoni, E.; Bernardini, M.G.; Margutti, R.; Amati, L. Update on the GRB universal scaling $E_{X,iso}$-$E_{\gamma,iso}$-E_{pk} with 10 years of Swift data. *Mon. Not. R. Astr. Soc.* **2016**, *455*, 1375–1384.
253. Kouveliotou, C.; Woosley, S.E.; Patel, S.K.; Levan, A.; Blandford, R.; Ramirez-Ruiz, E.; Wijers, R.A.M.J.; Weisskopf, M.C.; Tennant, A.; Pian, E.; et al. Chandra Observations of the X-ray Environs of SN 1998bw/GRB 980425. *Astrophys. J.* **2004**, *608*, 872–882.
254. De Pasquale, M.; Piro, L.; Gendre, B.; Amati, L.; Antonelli, L.A.; Costa, E.; Feroci, M.; Frontera, F.; Nicastro, L.; Soffitta, P.; et al. The BeppoSAX catalog of GRB X-ray afterglow observations. *Astron. Astrophys.* **2006**, *455*, 813–824. [CrossRef]
255. Nysewander, M.; Fruchter, A.S.; Pe'er, A. A Comparison of the Afterglows of Short- and Long-duration Gamma-ray Bursts. *Astrophys. J.* **2009**, *701*, 824–836.
256. D'Avanzo, P.; Salvaterra, R.; Sbarufatti, B.; Nava, L.; Melandri, A.; Bernardini, M.G.; Campana, S.; Covino, S.; Fugazza, D.; Ghirlanda, G.; et al. A complete sample of bright Swift Gamma-ray bursts: X-ray afterglow luminosity and its correlation with the prompt emission. *Mon. Not. R. Astr. Soc.* **2012**, *425*, 506–513.
257. Oates, S.R.; Racusin, J.L.; De Pasquale, M.; Page, M.J.; Castro-Tirado, A.J.; Gorosabel, J.; Smith, P.J.; Breeveld, A.A.; Kuin, N.P.M. Exploring the canonical behaviour of long gamma-ray bursts using an intrinsic multiwavelength afterglow correlation. *Mon. Not. R. Astr. Soc.* **2015**, *453*, 4121–4135.
258. Amati, L. The $E_{p,i}$-E_{iso} correlation in gamma-ray bursts: updated observational status, re-analysis and main implications. *Mon. Not. R. Astr. Soc.* **2006**, *372*, 233–245.
259. Jakobsson, P.; Hjorth, J.; Fynbo, J.P.U.; Watson, D.; Pedersen, K.; Björnsson, G.; Gorosabel, J. Swift Identification of Dark Gamma-Ray Bursts. *Astrophys. J. Lett.* **2004**, *617*, L21–L24.
260. Gehrels, N.; Barthelmy, S.D.; Burrows, D.N.; Cannizzo, J.K.; Chincarini, G.; Fenimore, E.; Kouveliotou, C.; O'Brien, P.; Palmer, D.M.; Racusin, J.; et al. Correlations of Prompt and Afterglow Emission in Swift Long and Short Gamma-Ray Bursts. *Astrophys. J.* **2008**, *689*, 1161–1172.
261. Berger, E. Short-Duration Gamma-Ray Bursts. *Ann. Rev. Astron. Astrophys.* **2014**, *52*, 43–105.
262. Wang, F.Y.; Dai, Z.G.; Liang, E.W. Gamma-ray burst cosmology. *New Astron. Rev.* **2015**, *67*, 1–17. [CrossRef]
263. Dainotti, M.G.; Del Vecchio, R. Gamma Ray Burst afterglow and prompt-afterglow relations: An overview. *New Astonomy Rev.* **2017**, *77*, 23–61.
264. Dainotti, M.G.; Del Vecchio, R.; Tarnopolski, M. Gamma-Ray Burst Prompt Correlations. *Adv. Astron.* **2018**, *2018*, 4969503. [CrossRef]
265. Wang, F.; Zou, Y.C.; Liu, F.; Liao, B.; Liu, Y.; Chai, Y.; Xia, L. A Comprehensive Statistical Study of Gamma-Ray Bursts. *Astrophys. J.* **2020**, *893*, 77.
266. Panaitescu, A.; Vestrand, W.T. Taxonomy of gamma-ray burst optical light curves: identification of a salient class of early afterglows. *Mon. Not. R. Astr. Soc.* **2008**, *387*, 497–504.
267. Panaitescu, A.; Vestrand, W.T.; Woźniak, P. Peaks of optical and X-ray afterglow light curves. *Mon. Not. R. Astr. Soc.* **2013**, *433*, 759–770.
268. Dainotti, M.G.; Livermore, S.; Kann, D.A.; Li, L.; Oates, S.; Yi, S.; Zhang, B.; Gendre, B.; Cenko, B.; Fraija, N. The Optical Luminosity-Time Correlation for More than 100 Gamma-Ray Burst Afterglows. *Astrophys. J. Lett.* **2020**, *905*, L26.
269. Dainotti, M.G.; Young, S.; Li, L.; Levine, D.; Kalinowski, K.K.; Kann, D.A.; Tran, B.; Zambrano-Tapia, L.; Zambrano-Tapia, A.; Cenko, S.B.; et al. The Optical Two- and Three-dimensional Fundamental Plane Correlations for Nearly 180 Gamma-Ray Burst Afterglows with Swift/UVOT, RATIR, and the Subaru Telescope. *Astrophys. J. Suppl.* **2022**, *261*, 25.
270. Dainotti, M.G.; Cardone, V.F.; Capozziello, S. A time-luminosity correlation for γ-ray bursts in the X-rays. *Mon. Not. R. Astr. Soc.* **2008**, *391*, L79–L83.
271. Ghisellini, G.; Nardini, M.; Ghirlanda, G.; Celotti, A. A unifying view of gamma-ray burst afterglows. *Mon. Not. R. Astr. Soc.* **2009**, *393*, 253–271.

272. Dainotti, M.G.; Willingale, R.; Capozziello, S.; Fabrizio Cardone, V.; Ostrowski, M. Discovery of a Tight Correlation for Gamma-ray Burst Afterglows with "Canonical" Light Curves. *Astrophys. J. Lett.* **2010**, *722*, L215–L219.
273. Dainotti, M.G.; Petrosian, V.; Singal, J.; Ostrowski, M. Determination of the Intrinsic Luminosity Time Correlation in the X-ray Afterglows of Gamma-Ray Bursts. *Astrophys. J.* **2013**, *774*, 157.
274. Dainotti, M.G.; Omodei, N.; Srinivasaragavan, G.P.; Vianello, G.; Willingale, R.; O'Brien, P.; Nagataki, S.; Petrosian, V.; Nuygen, Z.; Hernandez, X.; et al. On the Existence of the Plateau Emission in High-energy Gamma-Ray Burst Light Curves Observed by Fermi-LAT. *Astrophys. J. Suppl.* **2021**, *255*, 13.
275. van Eerten, H. Self-similar relativistic blast waves with energy injection. *Mon. Not. R. Astr. Soc.* **2014**, *442*, 3495–3510.
276. van Eerten, H.J. Gamma-ray burst afterglow plateau break time-luminosity correlations favour thick shell models over thin shell models. *Mon. Not. R. Astr. Soc.* **2014**, *445*, 2414–2423.
277. Dai, Z.G.; Lu, T. Gamma-ray burst afterglows and evolution of postburst fireballs with energy injection from strongly magnetic millisecond pulsars. *Astron. Astrophys.* **1998**, *333*, L87–L90.
278. Metzger, B.D.; Giannios, D.; Thompson, T.A.; Bucciantini, N.; Quataert, E. The protomagnetar model for gamma-ray bursts. *Mon. Not. R. Astr. Soc.* **2011**, *413*, 2031–2056.
279. Wang, F.Y.; Hu, J.P.; Zhang, G.Q.; Dai, Z.G. Standardized Long Gamma-Ray Bursts as a Cosmic Distance Indicator. *Astrophys. J.* **2022**, *924*, 97.
280. Beniamini, P.; Duque, R.; Daigne, F.; Mochkovitch, R. X-ray plateaus in gamma-ray bursts' light curves from jets viewed slightly off-axis. *Mon. Not. R. Astron. Soc.* **2020**, *492*, 2847–2857.
281. Dainotti, M.G.; Postnikov, S.; Hernandez, X.; Ostrowski, M. A Fundamental Plane for Long Gamma-Ray Bursts with X-ray Plateaus. *Astrophys. J. Lett.* **2016**, *825*, L20.
282. Dainotti, M.G.; Hernandez, X.; Postnikov, S.; Nagataki, S.; O'brien, P.; Willingale, R.; Striegel, S. A Study of the Gamma-Ray Burst Fundamental Plane. *Astrophys. J.* **2017**, *848*, 88.
283. Racusin, J.L.; Oates, S.R.; de Pasquale, M.; Kocevski, D. A Correlation between the Intrinsic Brightness and Average Decay Rate of Gamma-Ray Burst X-ray Afterglow Light Curves. *Astrophys. J.* **2016**, *826*, 45.
284. Hinds, K-R, .; Oates, S.R.; Nicholl, M.; Patel, J.; Omodei, N.; Gompertz, B.; L., R.J.; Ryan, G. Evidence for a luminosity-decay correlation in GeV GRB light curves. *Mon. Not. R. Astr. Soc.* **2023**, *submitted*.
285. Phillips, M.M. The Absolute Magnitudes of Type IA Supernovae. *Astrophys. J. Lett.* **1993**, *413*, L105. [CrossRef]
286. Riess, A.G.; Yuan, W.; Macri, L.M.; Scolnic, D.; Brout, D.; Casertano, S.; Jones, D.O.; Murakami, Y.; Anand, G.S.; Breuval, L.; et al. A Comprehensive Measurement of the Local Value of the Hubble Constant with 1 km s^{-1} Mpc^{-1} Uncertainty from the Hubble Space Telescope and the SH0ES Team. *Astrophys. J. Lett.* **2022**, *934*, L7.
287. Schaefer, B.E. Gamma-Ray Burst Hubble Diagram to z = 4.5. *Astrophys. J. Lett.* **2003**, *583*, L67–L70.
288. Amati, L.; Guidorzi, C.; Frontera, F.; Della Valle, M.; Finelli, F.; Landi, R.; Montanari, E. Measuring the cosmological parameters with the $E_{p,i}$-E_{iso} correlation of gamma-ray bursts. *Mon. Not. R. Astr. Soc.* **2008**, *391*, 577–584.
289. Capozziello, S.; Izzo, L. Cosmography by gamma ray bursts. *Astron. Astrophys.* **2008**, *490*, 31–36. [CrossRef]
290. Liang, N.; Xiao, W.K.; Liu, Y.; Zhang, S.N. A Cosmology-Independent Calibration of Gamma-Ray Burst Luminosity Relations and the Hubble Diagram. *Astrophys. J.* **2008**, *685*, 354–360.
291. Wang, F.Y.; Dai, Z.G. Weak gravitational lensing effects on cosmological parameters and dark energy from gamma-ray bursts. *Astron. Astrophys.* **2011**, *536*, A96.
292. Izzo, L.; Muccino, M.; Zaninoni, E.; Amati, L.; Della Valle, M. New measurements of Ω_m from gamma-ray bursts. *Astron. Astrophys.* **2015**, *582*, A115.
293. Muccino, M.; Izzo, L.; Luongo, O.; Boshkayev, K.; Amati, L.; Della Valle, M.; Pisani, G.B.; Zaninoni, E. Tracing Dark Energy History with Gamma-Ray Bursts. *Astrophys. J.* **2021**, *908*, 181.
294. Cardone, V.F.; Capozziello, S.; Dainotti, M.G. An updated gamma-ray bursts Hubble diagram. *Mon. Not. R. Astr. Soc.* **2009**, *400*, 775–790.
295. Cardone, V.F.; Dainotti, M.G.; Capozziello, S.; Willingale, R. Constraining cosmological parameters by gamma-ray burst X-ray afterglow light curves. *Mon. Not. R. Astr. Soc.* **2010**, *408*, 1181–1186.
296. Postnikov, S.; Dainotti, M.G.; Hernandez, X.; Capozziello, S. Nonparametric Study of the Evolution of the Cosmological Equation of State with SNeIa, BAO, and High-redshift GRBs. *Astrophys. J.* **2014**, *783*, 126.
297. Dainotti, M.G.; Lenart, A.Ł.; Chraya, A.; Sarracino, G.; Nagataki, S.; Fraija, N.; Capozziello, S.; Bogdan, M. The gamma-ray bursts fundamental plane correlation as a cosmological tool. *Mon. Not. R. Astr. Soc.* **2023**, *518*, 2201–2240.